

Phylogeography of Jackson's Forest Lizard *Adolfus jacksoni* (Sauria: Lacertidae) Reveals Cryptic Diversity in the Highlands of East Africa

ELI GREENBAUM^{1,11}, STEPHANIE DOWELL BEER², DANIEL F. HUGHES¹, PHILIPP WAGNER^{3,4}, CHRISTOPHER G. ANDERSON⁵, CESAR O. VILLANUEVA¹, PATRICK K. MALONZA⁶, CHIFUNDERA KUSAMBA⁷, WANDEGE M. MUNINGA⁷, MWENEBATU M. ARISTOTE⁸, AND WILLIAM R. BRANCH^{9,10}

¹ Department of Biological Sciences, University of Texas at El Paso, 500 W. University Avenue, El Paso, TX 79968, USA

² US Fish and Wildlife Service, Northeast Fishery Center, PO Box 75, 308 Washington Avenue, Lamar, PA 16848, USA

³ Department of Biology, Villanova University, 800 Lancaster Avenue, Villanova, PA 19085, USA

⁴ Allwetterzoo, Sentruper Street 315, D48161, Münster, Germany

⁵ Department of Biology and Museum of Southwestern Biology, University of New Mexico, Albuquerque, NM 87131, USA

⁶ Herpetology Section, National Museums of Kenya, Museum Hill Road, PO Box 40658-00100, Nairobi, Kenya

⁷ Laboratoire d'Herpétologie, Département de Biologie, Centre de Recherche en Sciences Naturelles, Lwiro, République Démocratique du Congo

⁸ Institut Supérieur d'Écologie pour la Conservation de la Nature, Katana Campus, Sud Kivu, République Démocratique du Congo

⁹ Bayworld, PO Box 13147, Humewood 6013, South Africa

¹⁰ Department of Zoology, Nelson Mandela Metropolitan University, Port Elizabeth, South Africa

ABSTRACT: Jackson's Forest Lizard (*Adolfus jacksoni*) is widespread throughout the highlands of the Albertine Rift, southern Uganda, western and central Kenya, and northern Tanzania. To understand the population genetics and phylogenetic relationships of this widespread taxon, we sequenced two mitochondrial (16S and *cyt b*) and two nuclear (*c-mos* and *RAG1*) genes from multiple populations. Population genetics analyses suggested a high degree of genetic differentiation among *A. jacksoni* populations, reflecting the high-elevation montane "islands" that they inhabit. Populations connected by a network of mountain ranges generally showed lower levels of genetic partitioning than those isolated by low-elevation habitat. Results from phylogenetic analyses and additional morphological data indicated that *Adolfus jacksoni* occurs throughout the Albertine Rift, likely from the Kabobo Plateau to the Lendu Plateau of Democratic Republic of the Congo, as well as southern Uganda, Mt. Elgon, and the highlands of western Kenya on the western side of the Kenyan Rift. *Adolfus kibonotensis* is removed from the synonymy of the latter taxon, elevated to full species, and recognized from the central Kenyan highlands to northern Tanzania on the eastern side of the Kenyan Rift. A new *Adolfus* species is described from the Mathews Range in central Kenya.

Key words: *Adolfus mathewsensis* sp. nov.; Democratic Republic of Congo; Kenya; Montane forest; Phylogeny; Population genetics; Tanzania; Taxonomy; Uganda

THE LACERTID genus *Adolfus* is currently known from Central and East Africa, including *A. africanus* (mid- to low-elevation forests from Cameroon to Kenya), *A. alleni*, and *A. masavaensis* (montane grasslands of Kenya and Uganda), and *A. jacksoni*, which is known from the disjunct mid- to high-elevation forests, forest edges, and anthropogenically disturbed habitats in countries surrounding the Albertine Rift, and the highlands of western and central Kenya and northern Tanzania (Loveridge 1957; Köhler et al. 2003; Wagner et al. 2014; Spawls et al. 2018). Based on aberrant scale patterns, Lönnberg (1907) named the subspecies *Adolfus jacksoni kibonotensis* from Tanzania, but half a century later, Loveridge (1957) synonymized the taxon with *A. jacksoni*. Originally described as *Lacerta jacksonii* by Boulenger (1899), the species was not included in the resurrected genus *Adolfus* by Arnold (1973), who recognized *A. africanus* (the type species; Sternfeld 1912; Boulenger 1920), *A. alleni*, and *A. vauereselli*. In the morphology-based study of Arnold (1989a), *L. jacksoni* was transferred to the genus *Adolfus*, which was thought to be paraphyletic with respect to *Holaspis*. Arnold (1989a,b) considered *A. jacksoni* to be the most plesiomorphic member of the Equatorial African clade, which included the genera *Adolfus*, *Gastropholis*, and *Holaspis*, a finding consistent with morphological analyses of Harris et al. (1998).

Harris et al. (1998) also used three mitochondrial genes to infer a phylogeny of the Family Lacertidae, and recovered two samples of *Adolfus* (*A. africanus* and *A. jacksoni*) as sister taxa in a weakly supported clade of their neighboring tree. The following year, however, Harris (1999) combined data from the latter study with mostly overlapping data from Fu (1998) and found that the same two species of *Adolfus* were not supported as sister taxa. In another phylogenetic analysis of lacertids with more extensive data sets, Fu (2000) did not recover two species of *Adolfus* (*A. jacksoni* and *A. vauereselli*) as monophyletic, a finding consistent with Salvi et al. (2011), and the latter taxon was eventually designated as the type species of the genus *Congolacerta* (Greenbaum et al. 2011). Additional studies with nuclear data sets by Mayer and Pavlicev (2007) and Hipsley et al. (2009) included *A. jacksoni* only. Greenbaum et al. (2011) included multiple populations and species of *Adolfus*, and recovered a sister relationship between a clade of *A. jacksoni* and a clade including *A. cf. jacksoni* (Arusha, Tanzania) and *A. alleni*. A similar relationship was recovered by Wagner et al. (2014), who described *A. cf. alleni* populations from the Aberdares and Mt. Elgon as a new species, *A. masavaensis*.

Herein, we conduct population genetics analyses and infer a phylogeny of the genus *Adolfus* with additional samples of *A. jacksoni* and *A. cf. jacksoni* to resolve the taxonomic status of the latter taxon. We follow the General Lineage Concept (de Queiroz 1999, 2007), which recognizes species as

¹¹ CORRESPONDENCE: e-mail, egreenbaum2@utep.edu

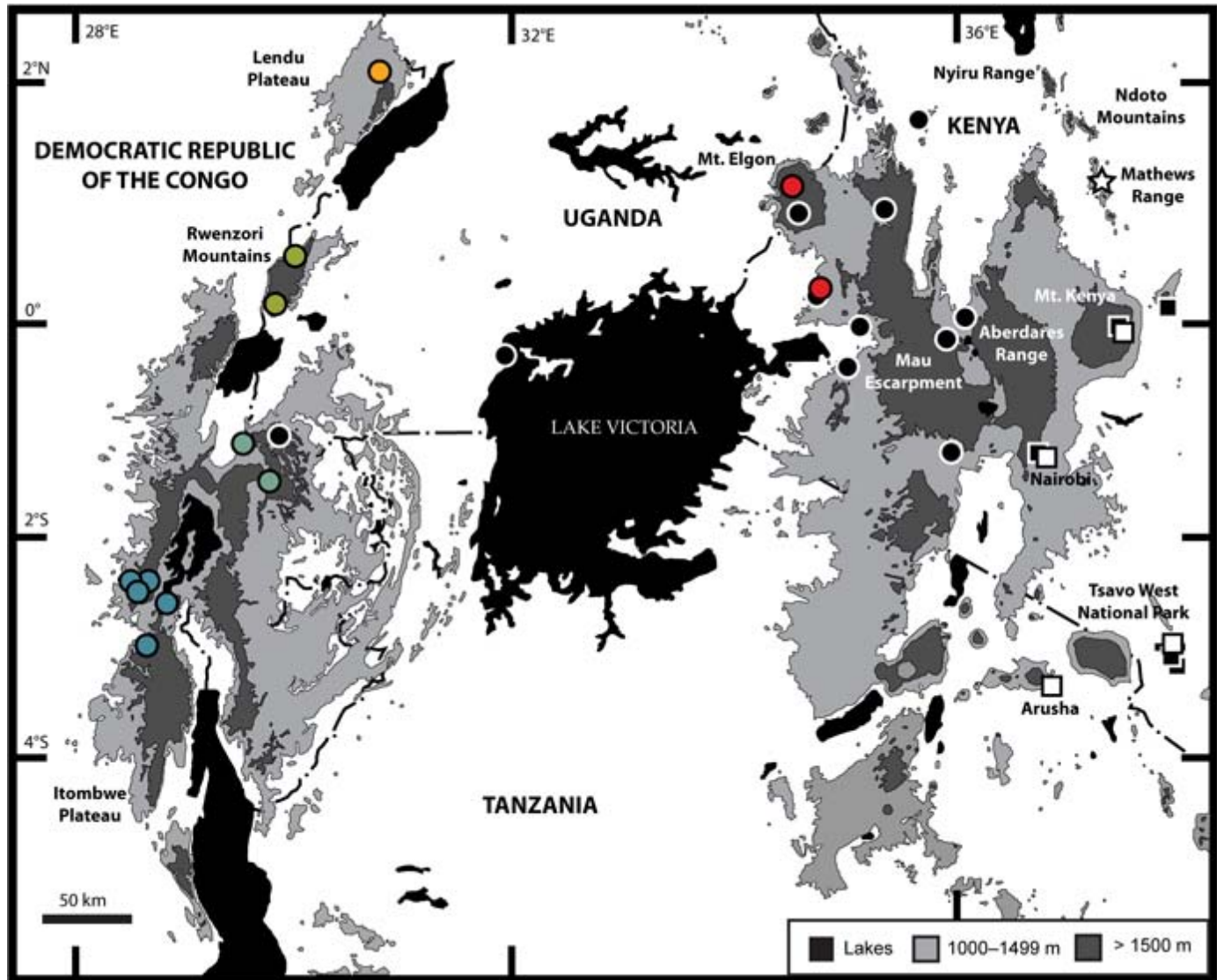


FIG. 1.—Map of the Albertine and Kenyan Rifts of Central and East Africa, showing genetic sampling localities for *Adolfus jacksoni* (open and colored circles), *A. kibonotensis* (open squares), and *A. matheusensis* (star). Colored circles for *A. jacksoni* samples match the color scheme shown in the haplotype network of Fig. 4. Closed (i.e., black) symbols represent localities for examined specimens that lack genetic data. A color version of this figure is available online.

separately evolving lineages. We reject the use of subspecies as natural groups and use molecular data sets to identify separately evolving species. Our species recognition criteria (Wiens and Penkrot 2002; de Queiroz 2007) are compatible with traditional morphological species that are diagnosed with unique morphological characters, including size, scale counts, and color pattern.

MATERIALS AND METHODS

Sampling

Several of the authors and their colleagues collected specimens and tissue samples (Appendix I) of *Adolfus* from eastern Democratic Republic of Congo (DRC) and proximate countries in East Africa (Fig. 1). Specimens were photographed in life, sampled for DNA tissues (95% ethanol), fixed in 10% buffered formalin, and transferred to 70% ethanol for long-term storage at the University of Texas at El Paso Biodiversity Collections (UTEP), National

Museums of Kenya (NMK), or Zoologisches Forschungsmuseum Alexander Koenig, Bonn, Germany (ZFMK). Additional examined specimens are shown in Appendix II, and we use the museum acronyms of Sabaj (2016). For latitude and longitude, we report World Geodetic System 1984 values.

Molecular Analyses

We sequenced two mitochondrial (16S and cytochrome *b* [*cyt b*]) and two nuclear (oocyte maturation factor [*c-mos*] and recombination activating gene 1 [*RAG1*]) genes from 11 specimens of *Adolfus jacksoni* and *A. cf. jacksoni*, and these data were combined with selected samples of previously sequenced lacertid data from Greenbaum et al. (2011) and Wagner et al. (2014), including the outgroups *Atlantolacerta andreanskyi* and *Iberolacerta cyreni*. We deposited newly sequenced samples for this study into GenBank (Appendix I).

TABLE 1.—Primer sequences used in this study.

Name	Source	Sequence	Gene
16SA-L	Palumbi et al. (1991)	5'-CGCCTGTTTATCAAAAACAT-3'	16S
16SB-H	Palumbi et al. (1991)	5'-CCGGTCTGAACTCAGATCACGT-3'	16S
CytbF700	Bauer et al. (2007)	5'-CTTCCAACACCAYCAAACATCTCAGCATGATGAAA-3'	cyt <i>b</i>
CytbR700	Bauer et al. (2007)	5'-ACTGTAGCCCCCTCAGAATGATATTTGTCCTCA-3'	cyt <i>b</i>
Hcmos3	Mayer and Pavlicev (2007)	5'-GGTGATGGCAAATGAGTAGAT-3'	c-mos
L-1zmos	Mayer and Pavlicev (2007)	5'-CTAGCTTGGTGTCTATAGACTGG-3'	c-mos
Hcmos1	Mayer and Pavlicev (2007)	5'-GCAAATGAGTAGATGTCTGCC-3'	c-mos
R13	Groth and Barrowclough (1999)	5'-TCTGAATGGAAATTCAAGCTGTT-3'	RAG1
R18	Groth and Barrowclough (1999)	5'-GATGCTGCCTCGGTCCGCCACCTTT-3'	RAG1
RAG1f700	Bauer et al. (2007)	5'-GGAGACATGGACACAATCCATCCTAC-3'	RAG1
RAG1r700	Bauer et al. (2007)	5'-TTTGTACTGAGATGGATCTTTTTGCA-3'	RAG1

We isolated genomic DNA from alcohol-preserved liver or muscle tissue samples with the Qiagen DNeasy tissue kit (Qiagen Inc.). We used 25 μ L polymerase chain reaction reactions with gene-specific primers (Table 1), with an initial denaturation step of 95°C for 2 min, followed by denaturation at 95°C for 35 s, annealing at 50°C for 35 s, and extension at 72°C for 95 s with 4 s added to the extension per cycle for 32 (mitochondrial genes) or 34 (nuclear genes) cycles. We visualized amplicons on a 1.5% agarose gel stained with SYBR Safe DNA gel stain (Invitrogen Corporation), purified target products with AMPure magnetic bead solution (Agencourt Bioscience) and sequenced them with BigDye® Terminator Cycle Sequencing Kits (Applied Biosystems). We purified sequencing reactions with CleanSeq magnetic bead solution (Agencourt Bioscience) and sequenced them with an ABI 3130xl automated sequencer at the Genomic Analysis Core Facility at UTEP. We assembled forward and reverse contiguous overlapping DNA segments for each sample and edited them using default parameters of SeqMan (v8.0.2, DNASTAR, Madison, WI; Swindell and Plasterer 1997) to ensure accuracy. One sample of *Adolfus jacksoni* (CAS 201598) showed evidence of pseudogenes (i.e., six codon insertion relative to all other lacertids with a reading frame shift) for c-mos; Pavlicev and Mayer (2006) also reported c-mos pseudogenes in three species of *Lacerta*. Our pseudogene sequence was excluded from the data set of this study. We produced an initial alignment of each gene with default parameters in MEGA-LIGN (v8.0.2, DNASTAR, Madison, WI) with the Clustal W algorithm (Thompson et al. 1994), and manual adjustments were made in MacClade v4.08 (Maddison and Maddison 2005). We translated protein-coding genes to amino acids with MacClade to confirm conservation of the amino-acid reading frame, ensure alignment, and check for premature stop codons. No ambiguously aligned regions were observed, and as a result, no data were excluded from phylogenetic analyses.

We assessed phylogenetic relationships among the samples with maximum-likelihood and Bayesian-inference optimality criteria in the programs RAxML v3.2.48 (Stamatakis 2006) and MrBayes v3.1 (Ronquist and Huelsenbeck 2003), respectively. The Akaike Information Criterion (Posada and Buckley 2004) in jModelTest 2 (Darriba et al. 2012) was used to find the model of evolution that best fit the data for subsequent analyses with MrBayes and BEAST. RAxML analyses were executed with partitioned data sets (one for 16S, and one for each codon position of all other protein-coding genes), and 100 replicate maximum-likeli-

hood inferences were performed for each analysis. Each analysis was initiated with a random starting tree, included the GTRGAMMA option (-m) and employed the rapid hill-climbing algorithm (-x; Stamatakis et al. 2007). Clade support was assessed with 1000 bootstrap replicates, with the rapid-hill climbing algorithm (Stamatakis et al. 2008), and branches receiving $\geq 95\%$ bootstrap support were considered to be well-supported (Wilcox et al. 2002).

We conducted partitioned Bayesian analyses with default priors. Analyses were initiated with random starting trees and run for 10,000,000 generations; Markov chains were sampled every 1000 generations. We checked convergence by importing the trace files (p files) from the MrBayes output to the computer program Tracer v1.3 (available at <http://tree.bio.ed.ac.uk/software/tracer/>), which plots the likelihood values against generation number. Once the graphical plot leveled off, convergence had been met; we conservatively discarded 25% of trees as burn-in. Four separate analyses with two independent chains were executed to check for convergence of log-likelihoods in stationarity (Huelsenbeck and Ronquist 2001). All phylogenetic trees were visualized with FigTree v1.4.1 (Rambaut and Drummond 2010). Nodes with posterior probabilities ≥ 0.95 were considered to be well-supported (Leaché and Reeder 2002; Wilcox et al. 2002). We inferred levels of sequence divergence between putative species by using uncorrected p-distances (proportion [p] of nucleotide sites at which two sequences being compared are different) calculated from MEGA v6.0 (Tamura et al. 2013).

For population-genetics analyses, two individuals, ZFMK 63267 and ZFMK 74512, were removed from the nuclear analyses because of a large proportion of missing sequence data. Haplotype reconstruction of the nuclear gene regions was carried out using PHASE (Stephens and Donnelly 2003) as implemented in DnaSP v5.10.1 (Librado and Rozas 2009). We visually assessed the degree of genetic differentiation among the *A. jacksoni* populations by constructing median-joining haplotype networks (Bandelt et al. 1999) for the mitochondrial data set and each nuclear gene region, with the software PopART v1.7 (Leigh and Bryant 2015). To examine the genetic subdivision further, we performed a population aggregation analysis (Davis and Nixon 1992), by extracting all variable sites with the web-based program FaBox v1.41 (available at <http://users-birc.au.dk/biopv/php/fabox/>). This analysis was performed only on the mitochondrial data set because of the larger degree of nucleotide variation. Population isolation is required for nucleotide fixation to occur; therefore, the population aggregation analysis can also provide an indication of the level of gene

TABLE 2.—Fossil-calibration priors used for estimating divergence dates in Fig. 5. The translated log-normal (TL) zero-offset is presented in millions of years ago (mya), parameter values (mean and standard deviation) are in parentheses, and posterior (calculated) ages are presented as median with 95% confidence interval in parentheses.

Node	TL zero-offset (mean, SD)	Median (95% CI)	Fossil source
1	238 (1.4, 0.7)	242.1 (239.3–250.8)	Fossil rhynchocephalian (Jones et al. 2013)
2	161 (1.8, 1.0)	167 (162.2–192.3)	<i>Balnealacerta</i> (Evans 1998)
3	111 (1.8, 1.3)	117 (111.5–162.3)	<i>Hodzhakulia</i> (Evans 2003)
4	70 (1.6, 0.8)	74.9 (71.3–88.5)	<i>Chamops</i> , <i>Haptosphenus</i> , <i>Letpochamops</i> , and <i>Meniscognathus</i> (Estes 1964; Bryant 1989; Denton and O'Neill 1995)
5	128 (1.0, 0.5)	131.3 (129–138.5)	<i>Dalinghosaurus longidigitus</i> (Evans and Wang 2005)
6	70 (1.8, 1.0)	76.1 (71.2–101.3)	<i>Odaxosaurus</i> (Sullivan and Lucas 1996)
7	70 (1.8, 1.0)	76.1 (71.2–101.3)	Priscagaminae (Keqin and Norell 2000)

flow occurring across *A. jacksoni* populations. To avoid biasing the results, we excluded regions with large gaps in sequence data.

We estimated population differentiation in the mitochondrial and nuclear data sets, including F_{ST} and the Φ_{ST} fixation indices, in Arlequin v3.5.2.2 (Excoffier and Lischer 2010) with 10,100 permutations to test for significance. Values of F_{ST} can be considered short-term genetic distances between populations, whereas the Φ_{ST} fixation index is based on haplotype frequencies (Excoffier and Lischer 2010).

We estimated divergence dates for *Adolfus* using a fossil-calibrated approach in the Bayesian program BEAST v1.8.4 (Drummond et al. 2012) on our multilocus data set. To achieve a robust representation of the Family Lacertidae, we included at least two species per genus when available on GenBank, and to maximize calibration points, we included 25 additional squamate taxa plus *Sphenodon punctatus* (Table S1 in the Supplemental Materials available online). For some distantly related lineages, chimeric sequences using more than one species from the same or a closely related genus were constructed (Zheng and Wiens 2016). Fossil calibrations were placed on seven nodes that correspond to some of the oldest known fossils of Lepidosauria (Table 2). For each calibration, we used a translated log-normal distribution with an offset equal to the age of the fossil. We chose an uncorrelated log-normal relaxed clock model with an estimated clock rate to allow for rate heterogeneity among lineages, and tree shape was estimated with the Yule prior because a constant speciation rate is assumed (Drummond et al. 2006). We estimated a chronogram from one run of 100 million generations, and trees were sampled every 5000 generations. The initial 10% of trees were discarded, and we summarized parameter values on the maximum clade credibility tree with TreeAnnotator. Tracer was used to confirm stationarity and adequate ESS of the posterior probabilities. Posterior probabilities $\geq 95\%$ were considered as strongly supported. Date analyses were run on the CIPRES Science Gateway v3.3 (available at <http://www.phylo.org/>).

Morphological Analyses

The specimens we examined for this study (Appendix II) were preserved in 10% buffered formalin in the field, and transferred to 70% ethanol at the conclusion of each expedition. Tissues were harvested before formalin fixation from the liver or hind limb muscle of lizards, and preserved in 95% ethanol. The first author recorded morphometric data from these preserved specimens with digital calipers to the nearest 0.1 mm under a stereomicroscope. Color descriptions

are based on preserved specimens, field notes, and color digital images in life. We determined sex by direct examination of gonads, or from the presence of everted hemipenes.

Meristic and mensural characters were chosen from lacertid studies by Arnold (1989b) and by Lue and Lin (2008), and are consistent with Greenbaum et al. (2011). Measurements were taken on the right side of the lizard and included snout–vent length (SVL, from tip of snout to anterior margin of vent); tail length (from posterior margin of vent to tail tip, measured only from specimens with complete and original tails); head length (from tip of snout to anterior margin of ear opening); maximum head width (measured at the broadest point); head height (measured at the rictus); skull length (from tip of snout to posterior margin of occipital); snout–eye length (from tip of snout to anterior margin of eye [i.e., anterior corner of the ocular aperture]); mouth length; snout–arm length (from tip of snout to anterior margin of forelimb); axilla–groin distance (from posterior edge of forelimb insertion to anterior edge of hind limb insertion); brachium length; antebrachium length; thigh length; shank length; and longest toe length (length of fourth toe on hind limb).

Meristic data were taken from the right side of each lizard, except for femoral pore counts if field or museum tags were tied to the right leg. Definition of scales follow those of Arnold (1989b) and Arnold et al. (2007), and include chin shields; femoral pores; supralabials (counted to rictus); infralabials (counted to rictus); supraoculars; supraciliaries (counted between the lateral edges of the supraoculars and the anterior–posterior margin of the ocular aperture [Peters 1964]); supraciliary granules; supratemporals; anterior dorsal scale rows (counted transversely at posterior insertion of forelimbs); posterior dorsal scale rows (counted transversely at anterior insertion of hind limbs); dorsal scale rows at midbody (counted transversely at midpoint between fore- and hind limbs); dorsal scale numbers (counted longitudinally from posterior margin of occipital to posterior margin of hind limbs); ventral rows (counted transversely at midbody); ventral scale numbers (counted longitudinally from posterior margin of collars to anterior margin of preanal scales; took average from the middle two rows); caudal scales (counted around the tail at the position of the 11th and 15th scale to avoid the difference between males and females); subdigital lamellae on fingers and toes (counted from the most proximal scale at the interdigital skin to the unguis scale); and number of vertebral scales (counted transversely within pale (tan, gray, or light brown) middorsal region (Fig. 2A) behind occipital and at midbody. In the description, we use a dash for ranges and a solidus (/) to report counts from the left and right sides of a single specimen.

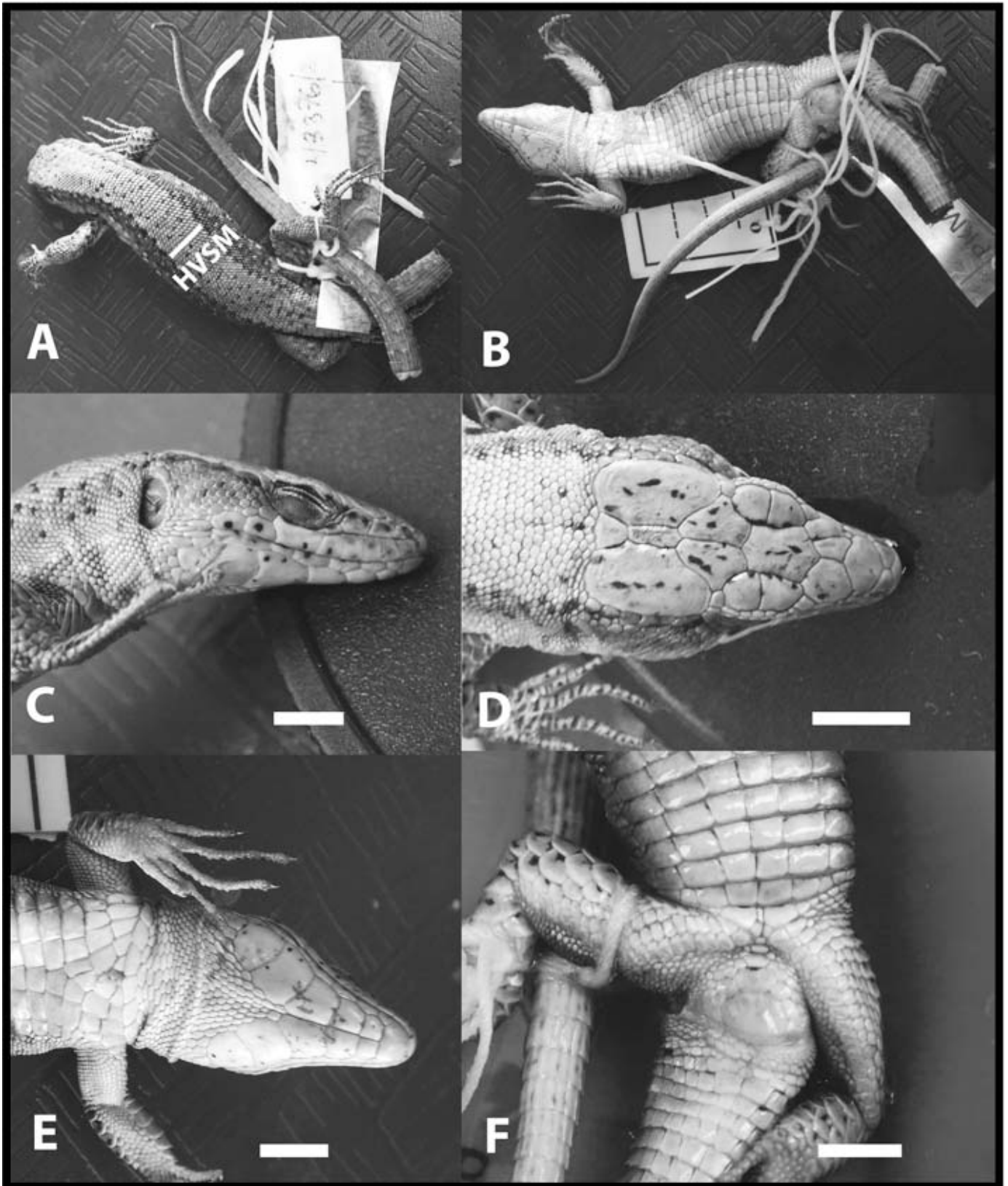


FIG. 2.—Photographs of the holotype of *Adolfus mathewsensis* (NMK L/3376/2, adult male, 68.75 mm snout–vent length) after preservation. (A) Dorsal view of whole specimen illustrating number of vertebral scales (counted horizontally) within pale middorsal region at midbody (HVSM); (B) ventral view of whole specimen; (C) lateral view of head; (D) dorsal view of head; (E) ventral view of head; and (F) ventral view of cloacal region illustrating femoral pores. Scale bars = 0.5 cm.

After verifying that our data satisfied assumptions of homogeneity and normality, we conducted statistical comparisons of selected measurements and meristic data with paired *t*-tests. To eliminate the effect of size for interspecific comparisons, we conducted an analysis of covariance with snout-vent length as the covariate (Packard and Boardman 1999). All statistical tests were run with Minitab (v14.20, Minitab Inc., State College, PA) and we adjusted the Type I significance level with the Bonferroni method.

RESULTS

Molecular Analyses

The 16S data did not include any ambiguous alignments, all other protein-coding genes were aligned by codon position, and we did not exclude any data from phylogenetic analyses. The final data set included 2413 base pairs (bp), including 16S (551 bp), *cyt b* (344 bp), *c-mos* (571 bp), and RAG1 (947 bp). The jModelTest 2 program selected the following models for the gene partitions: 16S = GTR+I+G; *cyt b* 1st codon = TIM2+H+G; *cyt b* 2nd codon = TrNef+I; *cyt b* 3rd codon = TIM2+I; *c-mos* 1st codon = K80+I; *c-mos* 2nd codon = TIM3ef; *c-mos* 3rd codon = K80+G; RAG1 1st codon = K80+G; RAG1 2nd codon = K80; RAG1 3rd codon = K80+G. The maximum-likelihood analysis likelihood score of the optimal tree was -9896.449. Tree topologies for the maximum-likelihood and Bayesian-inference analyses were identical, with similar, strong support values for most clades (Fig. 3). All samples of *Adolfus* were recovered in a strongly supported clade, and other strongly supported clades (both maximum-likelihood and Bayesian-inference analyses) within the genus included *A. africanus*, *A. kibonotensis* (a synonym of *A. jacksoni*), *A. alleni*, *A. masavaensis*, and *A. jacksoni*. A single sample of *Adolfus* from the Mathews Range of Kenya (NMK L/3376/2) was strongly supported as sister to *A. kibonotensis* in the Bayesian-inference analysis (maximum-likelihood bootstrap support 81%). Uncorrected *p*-distances between populations of *Adolfus alleni*, *A. jacksoni*, *A. kibonotensis*, *A. masavaensis*, and NMK L/3376/2 (Mathews Range) were moderate to high for mitochondrial genes (16S = 3.4–7.6%; *cyt b* = 12.2–14.9%) and low for nuclear genes (*c-mos* = 0.3–1.1; RAG1 = 0.5–1.8).

We noted one difference in amino acid translation of the *c-mos* gene at codon position 39 between all populations of *A. jacksoni* (histidine) and all other *Adolfus* samples (arginine), including NMK L/3376/2 (Mathews Range) and *A. kibonotensis*. We noted four differences in amino acid translation of the RAG1 gene between NMK L/3376/2, *A. kibonotensis*, and *A. jacksoni*. Amino-acid codon position 16 translated to serine for NMK L/3376/2, whereas the same position translated to asparagine in all other *Adolfus* populations. Amino-acid codon position 40 translated to isoleucine in NMK L/3376/2, whereas this codon position translated to methionine in all other *Adolfus* populations. Amino-acid codon position 65 translated to valine in all samples of *A. kibonotensis*, whereas the same position translated to alanine in NMK L/3376/2 and all *A. jacksoni* populations. Amino-acid codon position 204 translated to phenylalanine for NMK L/3376/2, whereas the same position translated to leucine in all other *Adolfus* populations.

Our median-joining haplotype networks revealed a large degree of genetic partitioning among the *A. jacksoni* populations (Fig. 4). For the mitochondrial network, each population formed a discrete cluster, connected to other populations by a single branch, reflecting limited gene flow. However, two populations, DRC and Rwanda, shared the same major branch, indicating a lower level of genetic isolation than among other populations. Additionally, no mitochondrial haplotypes were shared across populations. The RAG1 network showed a greater degree of variation than *c-mos*, which had only three total base-pair differences. Both nuclear median-joining networks showed a higher degree of connectivity than the mitochondrial network, with individuals from all localities, except the East population, sharing haplotypes for both *c-mos* and RAG1. In general, individuals from the East population, located on the eastern side of Lake Victoria, had a larger number of base-pair differences compared with those in the other populations.

Our population aggregation analysis was performed only on the mitochondrial data set because of the larger degree of nucleotide variation. From this analysis, we found that each population could be differentiated by multiple fixed nucleotide differences, indicative of population isolation (Fig. S1 in the Supplemental Materials available online). Fixed differences were observed in the East population at seven nucleotide positions (187, 242, 445, 658, 694, 763, and 809), in the Lendu Plateau population at eight positions (116, 244, 324, 373, 578, 667, 775, and 778), in the West Uganda population at seven positions (316, 323, 369, 379, 652, 766, and 787), in the Rwanda population at two positions (369 and 844), and in the DRC population at two positions (584 and 802). The DRC and Rwanda populations, together, shared 13 fixed nucleotide differences (positions 323, 324, 346, 357, 367, 370, 417, 515, 577, 608, 664, 712, 760) not present in the remaining populations. The F_{ST} and Φ_{ST} fixation indices showed statistically significant levels of genetic partitioning for comparisons involving both the East and DRC populations (Table 3).

Our calibrated dating analyses indicated that Lacertidae diverged around 120 million yr ago (mya; 106.51–139.55 mya, 95% highest posterior densities [HPD]) and the subfamily Gallotinae diverged from Lacertinae around 87 mya (71.69–104.44 mya, HPD; Fig. S2 in the Supplemental Materials available online). The genus *Adolfus* diverged from other lacertids in the Eocene at 45 mya (35.05–56.51 mya, HPD; Fig. 5). The initial divergence of *A. africanus* from the other species in the genus occurred in the mid-Oligocene at 28 mya (19.53–37.88 mya, HPD). The remaining *Adolfus* species originated in the Miocene with few HPDs ranging into the Pliocene. The divergence of the two major *Adolfus* clades was dated in the Miocene at 16 mya (12.00–22.07 mya, HPD). The divergence of *A. mathewsensis* (NMK L/3376/2, Mathews Range) from *A. kibonotensis* was estimated in the late Miocene at 11 mya (6.36–16.89 mya, HPD).

Morphological Analyses

Our morphological data for adult *Adolfus jacksoni*, *A. kibonotensis*, and *A. mathewsensis* are presented in Table 4. Among *A. jacksoni*, the only taxon with an adequate sample size of females ($n = 9$), males were larger than females for head length ($P < 0.001$), maximum head width ($P < 0.001$), head height ($P < 0.001$), skull length ($P < 0.001$), snout-eye

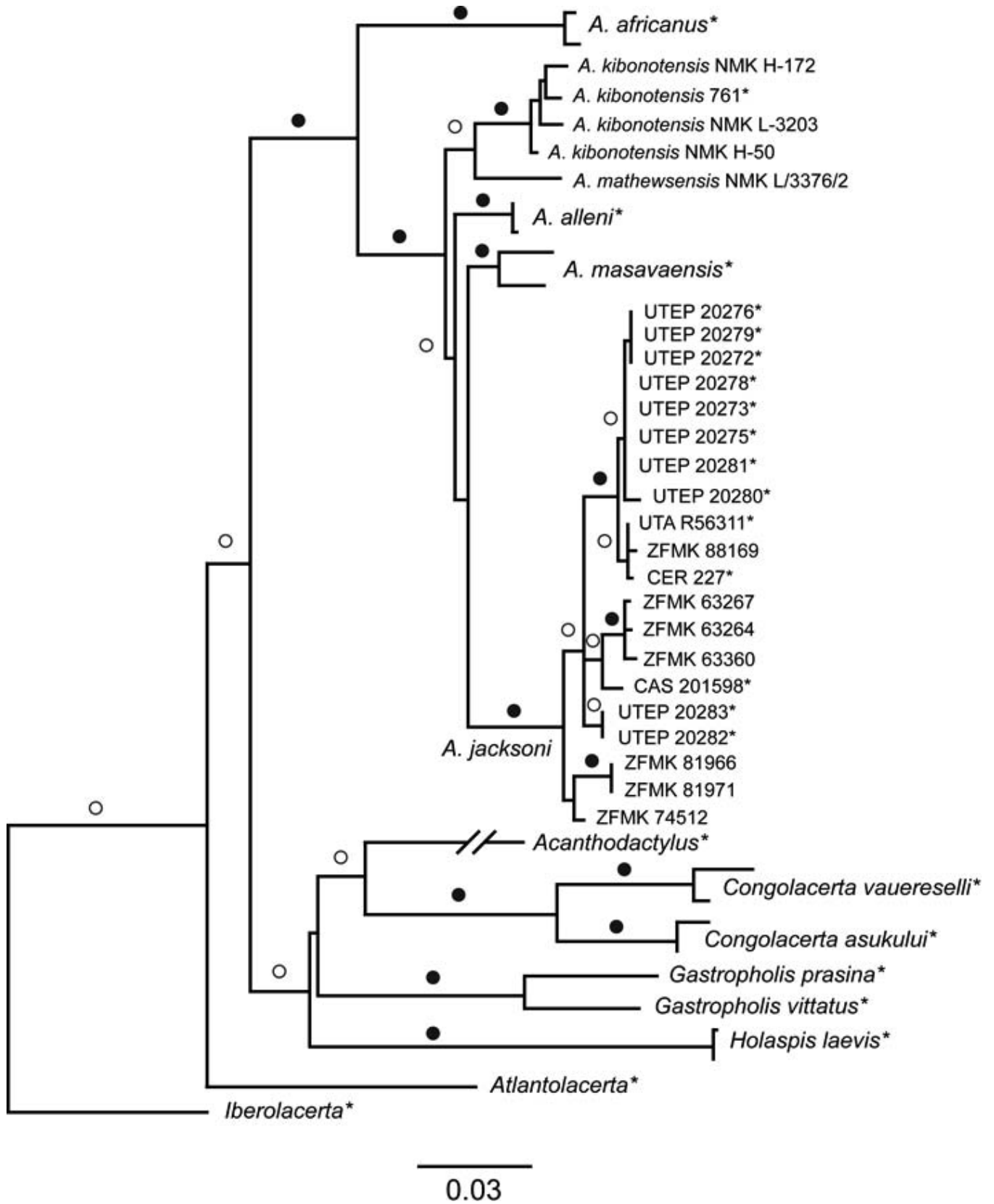


FIG. 3.—Maximum-likelihood phylogeny (RAxML tree) of the Equatorial African lacertids from Central and East Africa. Open circles represent nodes supported with high posterior probability values from Bayesian analyses (≥ 0.95), and closed circles represent nodes supported with both high posterior probability values from Bayesian-inference analyses (≥ 0.95) and maximum-likelihood bootstrap values ($\geq 95\%$). See Appendix I for abbreviations of samples sequenced in this study, and Greenbaum et al. (2011) and Wagner et al. (2014) for samples with asterisks.

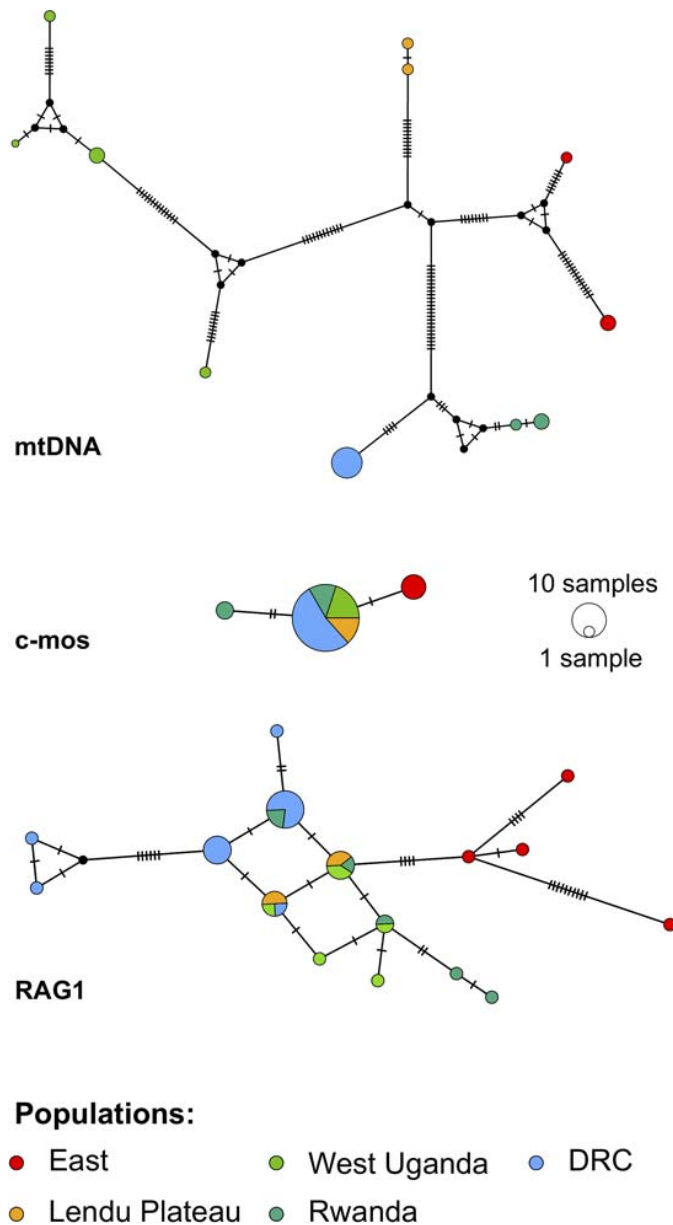


FIG. 4.—Median-joining haplotype networks created for populations of *Adolfus jacksoni*, based on the mitochondrial data set and nuclear gene regions (c-mos and RAG1). Circle sizes are proportional to the number of individuals and mutational steps are denoted by the hash marks. The colors represent the separate populations as indicated on the map (Fig. 1), and black circles designate hypothetical haplotypes. A color version of this figure is available online.

length ($P < 0.001$), mouth length ($P < 0.001$), snout–arm length ($P < 0.001$), thigh length ($P < 0.001$), and shank length ($P < 0.001$).

Our interspecific analysis of covariance (ANCOVA) detected no differences between male *A. jacksoni* and *A. kibonotensis*. However, male *A. jacksoni* had fewer supralabials ($P = 0.001$), supraciliary granules ($P = 0.001$), dorsal scale numbers ($P < 0.0001$), and number of vertebral scales at the middorsal region at midbody ($P = 0.001$) than male *A. kibonotensis*. Interspecific ANCOVA analyses between male *A. jacksoni* and *A. mathewsensis* identified a difference for axilla–groin distance ($P < 0.0001$). Male *A. jacksoni* had more dorsal scale numbers ($P < 0.0001$) and caudal scales at the 15th scale ($P = 0.001$) than male *A. mathewsensis*. Interspecific ANCOVA analyses did not identify differences between male *A. kibonotensis* and *A. mathewsensis*. However, male *A. kibonotensis* had fewer dorsal scale numbers ($P = 0.001$) and number of vertebral scales at the middorsal region at midbody ($P = 0.001$) than male *A. mathewsensis*.

Revised Taxonomy of *Adolfus jacksoni*

Based on records from Lönnberg (1907), Fischer and Hinkel (1992), Poblete (2002), and Spawls et al. (2018), and the combined results of our morphological and molecular data, we revise the taxonomy and distribution of East African *Adolfus* as follows. *Adolfus jacksoni* occurs from the Albertine Rift, likely from the Kabobo Plateau (Greenbaum and Kusamba 2012) to the Lendu Plateau, with sporadic records in southern Uganda, Rwanda, and northern Burundi to Mt. Elgon (Uganda–Kenya border), Kakamega Forest (Kenya), and the highlands of western Kenya west of the Kenyan (i.e., Gregorian) Rift. *Adolfus kibonotensis* (Fig. 6) is removed from the synonymy of the former taxon and elevated to full species status, and it occurs from Mombo (southwest of the West Usambara Mountains) and Mt. Kilimanjaro, Tanzania to the Taita Hills and south-central highlands of Kenya (including Mt. Kenya). A third taxon that is sister to *A. kibonotensis* is restricted to the Mathews Range of central Kenya, and is described as a new species below.

SPECIES DESCRIPTION

Adolfus mathewsensis sp. nov. (Figs. 2 and 6; Table 4)

Holotype.—An adult male (NMK L/3376/2, field No. PKM 0239, tissue No. PKM 0240) collected by P.K. Malonza on 10 June 2010, 1376 m above sea level (1.25140°N, 37.29332°E), between Ng'eny forest and Kitich Camp, Mugur Base Camp, Mathews Range North, Samburu County, Rift Valley Province, Kenya.

TABLE 3.—Pairwise F_{ST} and Φ_{ST} fixation index values among East African populations of *Adolfus jacksoni*, estimated with Arlequin. Values are based on the mitochondrial data set (above the diagonal) and nuclear data set (below the diagonal). DRC, the Democratic Republic of Congo. Bold values indicate significant values ($P < 0.05$) based on 10,100 permutations.

	F_{ST}					Φ_{ST}				
	East	Lendu Plat.	West Uganda	Rwanda	DRC	East	Lendu Plat.	West Uganda	Rwanda	DRC
East		0.683	0.611	0.798	0.903		0.208	0.148	0.167	0.325
Lendu Plateau	0.559		0.642	0.968	0.997	0.167		0.191	0.000	0.241
West Uganda	0.598	0.051		0.739	0.877	0.037	−0.081		0.000	0.191
Rwanda	0.530	0.184	0.106		0.973	0.037	0.111	−0.018		0.209
DRC	0.663	0.223	0.313	0.286		0.165	0.261	0.171	0.033	

TABLE 4.—Snout-vent length measurements (SVL, in mm), ratios (provided as percentages) and meristic data of adult specimens of *Adolfus jacksoni*, *A. kibonotensis*, and *A. mathewsensis*. Data are averages \pm 1 SD, with ranges in parentheses.

Characters	<i>A. jacksoni</i> (males, n = 21)	<i>A. kibonotensis</i> (males, n = 8)	<i>A. mathewsensis</i> (males, n = 4)	<i>A. jacksoni</i> (females, n = 9)	<i>A. kibonotensis</i> (females, n = 2)	<i>A. mathewsensis</i> (females, n = 1)
SVL	70.33 \pm 6.09 (60.6–84.3)	63.14 \pm 4.66 (57.2–71.6)	62.09 \pm 7.83 (51.7–68.8)	69.25 \pm 6.89 (55.4–76.6)	56.70, 63.67	60.64
Tail length/SVL	1.66 \pm 0.09 (1.58–1.76)	1.74	1.83	1.52	1.76, 1.51	—
Head length/SVL	0.26 \pm 0.01 (0.24–0.27)	0.25 \pm 0.01 (0.24–0.28)	0.24 \pm 0.01 (0.24–0.26)	0.20 \pm 0.02 (0.20–0.26)	0.22, 0.22	0.21
Head width/SVL	0.17 \pm 0.01 (0.15–0.21)	0.17 \pm 0.01 (0.15–0.18)	0.16 \pm 0.01 (0.15–0.17)	0.14 \pm 0.02 (0.12–0.18)	0.15, 0.15	0.14
Head height/SVL	0.12 \pm 0.01 (0.10–0.14)	0.12 \pm 0.01 (0.10–0.13)	0.10 \pm 0.01 (0.10–0.11)	0.09 \pm 0.01 (0.08–0.11)	0.10, 0.10	0.08
Skull length/SVL	0.26 \pm 0.01 (0.24–0.28)	0.26 \pm 0.01 (0.24–0.28)	0.25 \pm 0.01 (0.24–0.26)	0.21 \pm 0.02 (0.20–0.27)	0.23, 0.22	0.21
Snout-eye length/SVL	0.10 \pm 0.01 (0.09–0.12)	0.11 \pm 0.01 (0.09–0.11)	0.10 \pm 0.01 (0.09–0.10)	0.08 \pm 0.01 (0.08–0.10)	0.10, 0.10	0.09
Mouth length/SVL	0.20 \pm 0.02 (0.16–0.23)	0.21 \pm 0.01 (0.19–0.22)	0.20 \pm 0.02 (0.17–0.23)	0.16 \pm 0.02 (0.14–0.20)	0.20, 0.18	0.19
Snout-arm length/SVL	0.40 \pm 0.03 (0.35–0.44)	0.40 \pm 0.03 (0.35–0.44)	0.36 \pm 0.01 (0.35–0.36)	0.35 \pm 0.04 (0.31–0.45)	0.36, 0.34	0.36
Axilla-groin distance/SVL	0.43 \pm 0.03 (0.37–0.47)	0.43 \pm 0.03 (0.39–0.48)	0.47 \pm 0.03 (0.45–0.51)	0.50 \pm 0.04 (0.41–0.54)	0.44, 0.51	0.48
Brachium length/SVL	0.12 \pm 0.01 (0.09–0.14)	0.12 \pm 0.01 (0.10–0.13)	0.12 \pm 0.01 (0.11–0.13)	0.10 \pm 0.01 (0.09–0.12)	0.11, 0.11	0.11
Antebrachium length/SVL	0.12 \pm 0.01 (0.10–0.14)	0.12 \pm 0.01 (0.11–0.14)	0.11 \pm 0.00 (0.11)	0.10 \pm 0.01 (0.09–0.12)	0.11, 0.10	0.11
Thigh length/SVL	0.16 \pm 0.01 (0.13–0.19)	0.17 \pm 0.01 (0.15–0.20)	0.17 \pm 0.01 (0.16–0.19)	0.14 \pm 0.02 (0.12–0.17)	0.16, 0.13	0.15
Shank length/SVL	0.15 \pm 0.01 (0.14–0.17)	0.16 \pm 0.01 (0.15–0.18)	0.16 \pm 0.00 (0.16)	0.13 \pm 0.01 (0.12–0.16)	0.15, 0.13	0.15
Longest toe length/SVL	0.16 \pm 0.01 (0.14–0.18)	0.19 \pm 0.02 (0.16–0.21)	0.17 \pm 0.00 (0.16–0.17)	0.15 \pm 0.02 (0.11–0.20)	0.18, 0.15	0.16
Chin shields	5.48 \pm 0.51 (5–6)	5	5	5.67 \pm 0.50 (5–6)	5	5
Femoral pores	17.68 \pm 1.56 (15–21)	17.64 \pm 1.11 (16–20)	18.67 \pm 0.58 (18–19)	17.25 \pm 0.89 (16–18)	19, 17	17
Supralabials	6.50 \pm 0.59 (6–8)	7.44 \pm 0.50 (7–8)	7.50 \pm 0.58 (7–8)	6.44 \pm 0.73 (6–8)	7	7
Infralabials	6.05 \pm 0.22 (6–7)	6	6	6	6	6
Supraciliaries	4.05 \pm 0.22 (4–5)	4	4	4	4	4
Supraoculars	5.17 \pm 0.48 (4–6)	5.94 \pm 0.56 (5–7)	5.50 \pm 0.58 (5–6)	4.90 \pm 0.33 (4–5)	7, 5	5
Supraciliary granules	4.13 \pm 1.00 (2–6)	5.75 \pm 0.89 (5–7)	4.25 \pm 0.50 (4–5)	4.00 \pm 1.12 (2–5)	5, 4	5
Supratemporals	5.55 \pm 1.18 (4–8)	5.13 \pm 1.25 (3–7)	5.75 \pm 0.96 (5–7)	4.89 \pm 1.05 (3–6)	5	4
Anterior dorsal scale rows	64.10 \pm 7.01 (51–77)	62.00 \pm 4.44 (58–70)	62.75 \pm 5.06 (57–69)	62.75 \pm 6.55 (54–74)	48, 55	56
Posterior dorsal scale rows	42.43 \pm 3.12 (37–51)	41.13 \pm 2.36 (38–45)	41.00 \pm 2.16 (38–43)	40.33 \pm 2.87 (37–45)	37	40
Dorsal scale rows at midbody	43.62 \pm 3.22 (38–52)	41.25 \pm 2.19 (38–44)	41.75 \pm 1.50 (40–43)	40.11 \pm 3.18 (35–45)	37	39
Dorsal scale numbers	96.86 \pm 1.05 (90–106)	76.38 \pm 4.50 (70–83)	86.25 \pm 2.63 (84–90)	98.67 \pm 4.03 (93–105)	75, 79	85
Ventral rows	6	6	6	6	6	6
Ventral scale numbers	27.00 \pm 1.87 (24–32)	27.63 \pm 1.16 (26–29)	29.50 \pm 1.00 (29–31)	29.67 \pm 1.73 (27–32)	31	32
Caudal scales at 11th scale	24.95 \pm 1.61 (22–28)	24.50 \pm 1.52 (22–26)	22.50 \pm 2.52 (20–26)	24.00 \pm 1.10 (22–25)	21, 22	22
Caudal scales at 15th scale	24.16 \pm 1.61 (21–28)	22.60 \pm 0.89 (22–24)	20.50 \pm 1.00 (20–22)	23.80 \pm 1.10 (22–25)	22, 20	21
Subdigital lamellae on Finger 1	8.55 \pm 0.59 (8–10)	9.06 \pm 0.78 (8–10)	8.50 \pm 1.00 (7–9)	8.44 \pm 0.88 (7–10)	10, 8	9
Subdigital lamellae on Finger 2	13.64 \pm 0.91 (12–15)	14.38 \pm 0.92 (13–16)	13.50 \pm 0.58 (13–14)	13.44 \pm 0.88 (12–15)	14	12
Subdigital lamellae on Finger 3	18.36 \pm 1.04 (17–20)	19.44 \pm 1.40 (18–22)	17.50 \pm 0.58 (17–18)	17.78 \pm 1.20 (16–20)	17, 18	17
Subdigital lamellae on Finger 4	19.81 \pm 1.28 (18–22)	21.43 \pm 1.27 (19–23)	18.50 \pm 2.38 (17–22)	18.63 \pm 1.19 (17–21)	18, 21	18
Subdigital lamellae on Finger 5	12.86 \pm 1.12 (11–14)	13.44 \pm 0.73 (13–15)	12.50 \pm 1.00 (12–14)	12.67 \pm 1.12 (11–14)	15, 13	13
Subdigital lamellae on Toe 1	9.17 \pm 0.80 (7–10)	9.00 \pm 1.00 (8–10)	9.25 \pm 0.96 (8–10)	8.89 \pm 1.45 (6–11)	9, 10	9
Subdigital lamellae on Toe 2	14.05 \pm 0.96 (13–16)	14.00 \pm 2.16 (12–17)	14.00 \pm 0.82 (13–15)	13.67 \pm 1.32 (11–15)	15, 13	14
Subdigital lamellae on Toe 3	18.94 \pm 1.43 (16–21)	19.43 \pm 1.13 (18–21)	18.00 \pm 0.82 (17–19)	18.13 \pm 1.46 (16–20)	19, 18	17
Subdigital lamellae on Toe 4	23.86 \pm 1.88 (21–27)	24.14 \pm 1.35 (22–26)	23.25 \pm 1.89 (22–26)	22.89 \pm 1.45 (21–26)	25, 24	23
Subdigital lamellae on Toe 5	16.38 \pm 1.04 (15–18)	16.43 \pm 0.79 (16–18)	15.75 \pm 0.96 (15–17)	15.67 \pm 1.00 (14–17)	17, 16	16
Number of vertebral scales within pale middorsal region behind occipital	20.33 \pm 3.33 (16–25)	16.33 \pm 1.51 (14–18)	15.75 \pm 0.96 (15–17)	20.00 \pm 2.00 (19–23)	15	17
Number of vertebral scales within pale middorsal region at midbody	13.67 \pm 1.51 (12–16)	9.67 \pm 1.03 (8–11)	12.25 \pm 0.50 (12–13)	12.25 \pm 0.96 (11–13)	10	10

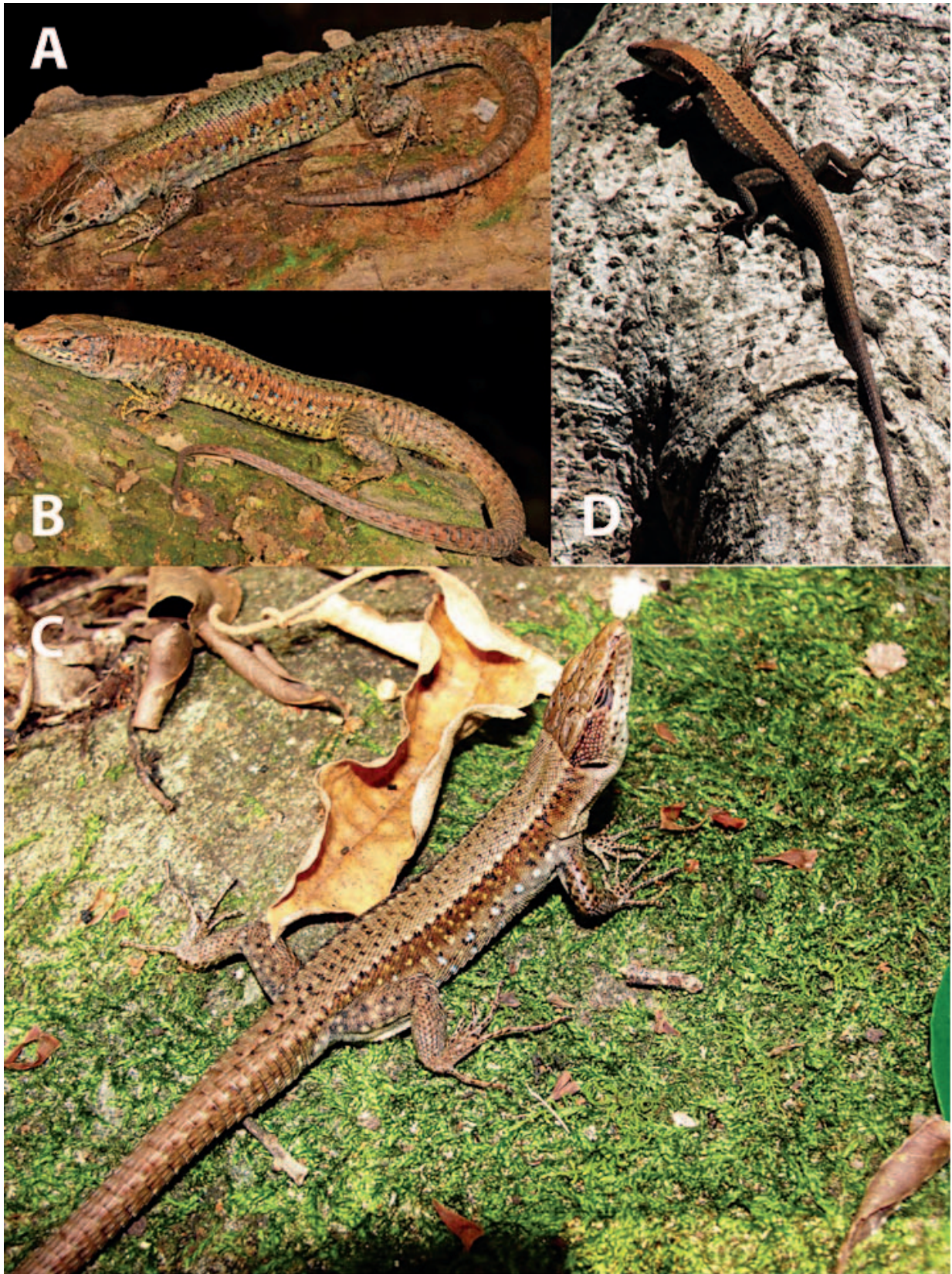


FIG. 6.—Photographs of *Adolfus kibonotensis* and *A. matheusensis* in life. (A) and (B) Dorsolateral view of *Adolfus kibonotensis* (specimen not collected) from Arusha, Tanzania. Photos by W.R. Branch. (C) Dorsolateral view of *Adolfus matheusensis* holotype (NMK L/3376/2, SVL 68.75 mm); and (D) dorsal view of uncollected specimen of *A. matheusensis*, in situ on a tree. Photos by P.K. Malonza.

32 ventral scale numbers (22–24), 20–26 caudal scales at the 11th scale row (14–16), 20–22 caudal scales at the 15th scale rows (14–16), 17–22 subdigital lamellae on Finger 4 (16–18), 12–14 subdigital lamellae on Finger 5 (11 or 12), 17–19 subdigital lamellae on Toe 3 (15–17), 22–26 subdigital lamellae on Toe 4 (18–20), 15–17 subdigital lamellae on Toe 5 (13–15), vertebral scales that are about the same size as those on the flanks (vertebral scales distinctly larger than those on the flanks), and presence of a pale (tan, gray or light brown) middorsal stripe (absent; Wagner et al. 2014).

Unlike *Adolfus alleni*, the new species has 17–19 femoral pores on each side (11–13), 5 or 6 supraciliaries (3–5), 4–7 supratemporals (2 or 3), 56–69 anterior dorsal scale rows (25–55), 38–43 posterior dorsal scale rows (17–23), 39–43 dorsal scale rows at midbody (18–23), 84–90 dorsal scale numbers (45–55), 12–14 subdigital lamellae on Finger 2 (10 or 11), 17 or 18 subdigital lamellae on Finger 3 (12–15), 17–22 subdigital lamellae on Finger 4 (14–16), 12–14 subdigital lamellae on Finger 5 (9 or 10), 13–15 subdigital lamellae on Toe 2 (9–11), 17–19 subdigital lamellae on Toe 3 (13–16), 22–26 subdigital lamellae on Toe 4 (17–20), 15–17 subdigital lamellae on Toe 5 (10–13), presence of supraciliary granules (absent), and presence of granules beneath the collar (absent; Wagner et al. 2014).

Unlike *Adolfus masavaensis*, the new species has 5 or 6 supraciliaries (3–5), 4–7 supratemporals (2 or 3), 56–69 anterior dorsal scale rows (23–49), 38–43 posterior dorsal scale rows (19–24), 39–43 dorsal scale rows at midbody (19–23), 84–90 dorsal scale numbers (42–57), 12–14 subdigital lamellae on Finger 2 (8–12), 17 or 18 subdigital lamellae on Finger 3 (11–14), 17–22 subdigital lamellae on Finger 4 (11–16), 12–14 subdigital lamellae on Finger 5 (8–10), 13–15 subdigital lamellae on Toe 2 (9–12), 17–19 subdigital lamellae on Toe 3 (12–16), 22–26 subdigital lamellae on Toe 4 (15–21), 15–17 subdigital lamellae on Toe 5 (10–15), presence of supraciliary granules (absent), and presence of granules beneath the collar (absent; Wagner et al. 2014).

Unlike *Adolfus jacksoni*, the new species has 84–90 dorsal scale numbers (90–106), and between conspecific males, fewer caudal scales at the 15th row ($P = 0.001$; Table 4).

Unlike *Adolfus kibonotensis*, the new species has 84–90 dorsal scale numbers (70–83), and between conspecific males, more dorsal scale numbers ($P = 0.001$) and number of vertebral scales at the middorsal region at midbody ($P = 0.001$; Table 4).

Description of the holotype.—An adult male with a long, but regenerated tail. Rostral separated from frontonasal by supranasals; nostril surrounded by supranasal, postnasal and first supralabial; supralabials eight (sixth largest) and infralabials six on each side; supraoculars four on each side, the anterior-most and posterior-most ones much smaller than others; supraciliaries six on each side, first supraciliary largest and continuing to dorsum of head to contact first two supraoculars, relative lengths $1 > 2 > 6 > 5 > 4 > 3$; second supraciliary in contact with second supraocular, posterior four supraciliaries and posterior half of second supraciliary separated from posterior supraoculars by five supraciliary granules on each side; postnasal one, followed by two loreals at each side, anterior loreal smaller than posterior one; prefrontals paired, although left prefrontal longitudinally divided; frontal hexagonal, contacting prefrontals, largest supraoculars, and frontoparietals; frontoparietals two and

connected; parietals two, separated by interparietal and occipital; supratemporals five on each side, first one largest on left, second one largest on right; temporal scales nonimbricate, much larger than scales posterior to ear opening; six pairs of chin shields, anterior-most three pairs in contact medially; gular fold present, contacting inferior edge of ear opening on left side; collar with eight plates, granules present beneath collar; dorsal scales on body enlarged, imbricate, keeled and rhombic, extending anteriorly beyond forelimbs on to neck, slightly larger than lateral scales at midbody, much larger than lateral scales near limb insertions; anterior dorsal scale rows 69, posterior dorsal scale rows 41, scale rows at midbody 43; scales counted longitudinally from occipital to the posterior margin of hind limb on middle-left and middle-right rows 84/84; lateral body scales at midbody keeled and rhombic, arranged in transverse rows; lateral body scales at limb insertions small, smooth or weakly keeled, and granular, arranged in disorder; small postfemoral mite pockets present; ventral scales rectangular, smooth, in six longitudinal rows at midbody, median and outer longitudinal rows smaller than others, outermost rows incomplete and smooth; scales counted longitudinally from posterior margin of collars to anterior margin of first preanal on middlemost two rows 29/30; two preanal scales, anterior-most smallest, ovoid, enlarged and smooth; femoral pores 19/19; scales on dorsal surfaces of forelimbs and hind limbs mostly enlarged, smooth and imbricate; scales on ventral surfaces of forelimbs mostly small and imbricate; relative lengths of appressed fingers $IV > III > V = II > I$; subdigital lamellae 10/9; 15/14, 18/18, 22/22, 14/14 on fingers I, II, III, IV and V, respectively; relative lengths of appressed toes $IV > III > V > II > I$; subdigital lamellae 10/10; 15/15, 19/19, 25/26, 17/17 on toes I, II, III, IV, and V, respectively; tail long and partially regenerated, covered with strongly keeled scales on lateral and dorsal sides, in 39 rows at base, decreased to 22 rows at 15th scale.

Measurements (in mm) of the holotype are as follows: snout–vent length 68.75; head length 16.36; head width 11.37; head height 6.79; skull length 16.55; snout–eye length 6.55; mouth length 14.15; tail length 110.64 (partially regenerated); snout–arm length 24.57; axilla–groin distance 34.88; brachium length 7.88; antibrachium length 7.81; thigh length 12.69; shank length 10.79; longest (4th) toe length 11.37.

From a photograph (Fig. 6C) before preservation: Dorsal ground color in the middorsal area from occipitals onto the tail is light brown to tan with numerous dark brown spots sprinkled throughout. A narrow, irregular line of dark brown spots interspersed with cream spots separates the middorsal area from the upper half of the flanks, which are brown to rusty brown with dark brown and white spots from the area posterior to the eye, through the ear opening to the insertion of the hind limbs. The latter area gradually blends into a light brown to tan ground color on the lower half of the flanks, and includes dark brown, cream, and light blue spots. The dorsum of the head, loreal region from the snout to the anterior of the eye and the limbs are brown to rusty brown with irregular dark brown blotches. The lateral side of the snout and neck (below the brown to rusty brown area in the loreal region and behind the eye) is cream with dark brown

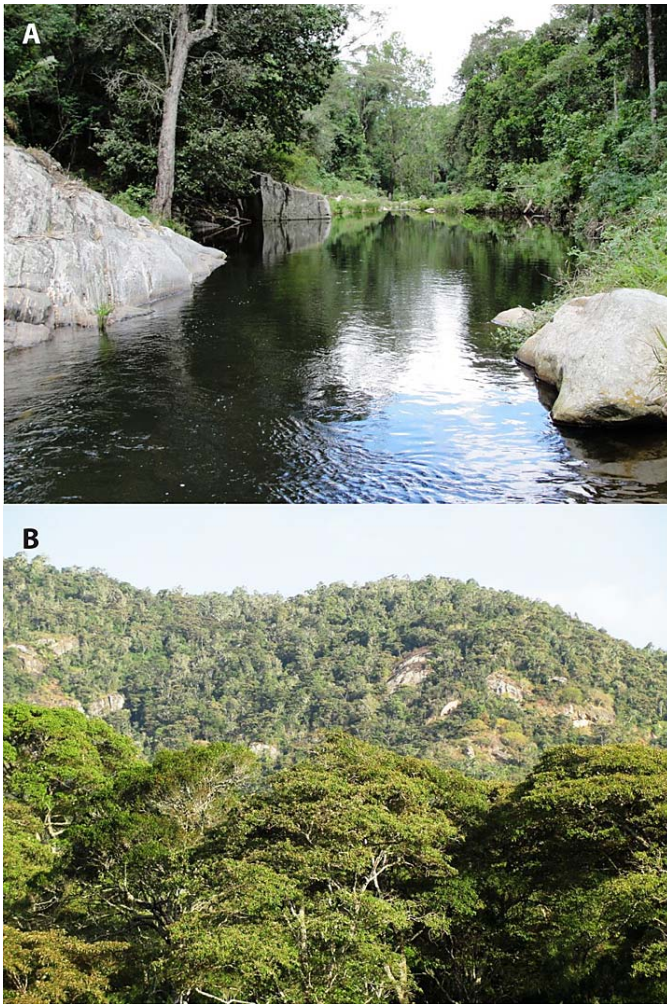


FIG. 7.—Habitats at the type locality for *Adolfus mathewsensis*. (A) Ng'eny River with granitic outcrops and gallery forest (1.2514°N, 37.2933°E, 1376 m, 9 June 2010); (B) Dry forest with granitic outcrops (1.1712°N, 37.3437°E, 1469 m, 3 June 2010). Photos by P.K. Malonza. A color version of this figure is available online.

blotches and spots. One small area of the venter on the underside of the right hind limb is cream.

Coloration of the holotype in 70% ethanol is similar to the coloration in life, except the light blue spots are cream, the lower half of the flanks are grayish blue, and the entirety of the venter is cream. Small dark brown spots are present on the chin shields. The femoral pores are yellowish.

Meristic and morphometric variation.—Variation of mensural and meristic data in the paratopotype and paratypes are shown in Table 4. In contrast to the holotype, all other type specimens have paired prefrontals that are not longitudinally divided. These specimens were not photographed in life, and their coloration in preservative is identical to that of the holotype. However, a photograph of an uncollected specimen (Fig. 6D) shows a more contrasting color pattern on the dorsum compared with the holotype.

Etymology.—The new name *mathewsensis* is an adjective meaning “from the Matthews Range,” where we discovered the new species.

Distribution and ecology.—Only known from the Mathews Range in east-central Kenya from 1376–1634 m

elevation. The new species was encountered basking on rocky outcrops adjacent to the Ng'eny River in gallery forest, and tree trunks, stems, and fallen trees in dry forest (Fig. 7). Other lizards found in these habitats included two species of geckos (*Cnemaspis* sp. and *Lygodactylus keniensis*) and a chameleon (*Trioceeros* sp.).

KEY TO SPECIES OF *ADOLFUS*

- 1a. Vertebral scales distinctly larger than those on flanks; outermost ventral scale rows incomplete and faintly keeled; venter lime green *A. africanus*
- 1b. Vertebral scales about same size as those on flanks; outermost ventral scale rows incomplete and smooth; venter not lime green 2
- 2a. Temporal scales large and few in number; no granular scales beneath collar; dorsal scale rows 18–24 at midbody 3
- 2b. Temporal scales small and numerous; granular scales present beneath collar; dorsal scale rows 35–52 at midbody 4
- 3a. Snout–vent length 38.9–55.5 mm; flanks dark brown to black; venter whitish; Mount Elgon and Aberdares *A. masavaensis*
- 3b. Snout–vent length 54.3–62.8 mm; flanks rufous; venter orange; Mount Kenya *A. alleni*
- 4a. Longitudinal dorsal scale rows >90; Albertine Rift to western Kenya *A. jacksoni*
- 4b. Longitudinal dorsal scale rows <90; Mathews Range, central Kenyan Highlands, or northern Tanzania 5
- 5a. Longitudinal dorsal scale rows 70–83; central Kenyan highlands to northern Tanzania *A. kibonotensis*
- 5b. Longitudinal dorsal scale rows 84–90; Mathews Range of Kenya *A. mathewsensis*

DISCUSSION

Our phylogenetic tree (Fig. 3) is consistent with other recent studies that focused on the Equatorial African group of lacertid lizards (Greenbaum et al. 2011; Wagner et al. 2014). Both of these studies supported a monophyletic group that includes the currently recognized species *A. africanus*, *A. alleni*, *A. kibonotensis*, *A. masavaensis*, *A. mathewsensis*, and *A. jacksoni*.

The intraspecific genetic analyses of *A. jacksoni* revealed highly disjunct populations. This population-level differentiation was evidenced by the fixed nucleotide differences among geographically disjointed populations of *A. jacksoni* that were observed in the mitochondrial haplotype network (Fig. 4) and population aggregation analysis (Fig. S1). The geography of the landscape seems to be the driving force behind the intraspecific patterns of *A. jacksoni* across their distribution. The more isolated populations, occurring in small patches of high-elevation islands surrounded by unsuitable low-elevation habitats, displayed a greater number of fixed nucleotide differences than those connected by a network of mountain ranges. For example, *A. jacksoni* populations in DRC and Rwanda showed lower levels of genetic isolation, with fixed nucleotide differences observed in only two positions, and we assigned both populations to the same major branch on the mitochondrial haplotype network. Additionally, these two populations shared 13 fixed

nucleotides not present in any other *A. jacksoni* population. In contrast, the geographically isolated *A. jacksoni* populations of the Lendu Plateau, West Uganda, and East groups, exhibited seven or eight private, fixed nucleotides each. This pattern of subdivision was consistent across other measures of genetic differentiation, with the same geographically fragmented populations (East, Lendu Plateau, and West Uganda) showing greater genetic differentiation than populations connected by proximate montane habitat (DRC and Rwanda).

Our estimated divergence dates for Lacertidae closely resemble analyses by Zheng and Wiens (2016), which included 52 genes and 4162 squamate species. Our recovered dates were older than previous estimations for the family (e.g., Hipsley et al. 2009; Pavlicev and Mayer 2009; Mendes et al. 2016), a finding corroborated by Zheng and Wiens (2016). We note that differences in methodological approaches among studies, including the use of fossil calibrations versus molecular rates, or large-scale sampling of most squamates versus small-scale sampling of terminal squamate groups, could have produced the discordance among the estimated divergence dates for Lacertidae (see Mendes et al. 2016, 2018). Nevertheless, we and others (e.g., Mendes et al. 2016; Zheng and Wiens 2016) have identified the Miocene epoch as an important period for diversification for the subfamily Lacertinae, and in particular, for East African *Adolfus* species. In the Miocene, the East African environment was undergoing significant changes derived from arid conditions induced by a combination of reduced atmospheric CO₂ concentrations globally (Cerling et al. 1997) and tectonic uplifts that altered climatic patterns (Sepulchre et al. 2006). Geological events and climatological shifts underlie trends of increased aridity and are associated with decreases in the extent of rainforest across sub-Saharan Africa in the Miocene (Kissling et al. 2012). Forest fragmentation during the Miocene likely underlie most of the species-level diversification patterns in *Adolfus*, including the new species *Adolfus mathewsensis*, a finding that is similar to other African squamates (e.g., Portillo et al. 2018). Several studies examined the phylogeography of amphibian and reptile groups that occur in the Albertine Rift (e.g., Greenbaum et al. 2012, 2013, 2015; Portillo et al. 2015; Larson et al. 2016; Hughes et al. 2017, 2018), but none have demonstrated a close affinity of Albertine Rift populations to those in Mt. Elgon and western Kenya, perhaps because of limited sampling in the latter areas. However, Kingdon (1990:166) remarked, "Mount Elgon especially seems to have drawn most of its fauna from the west." A limited number of studies have shown a close relationship between reptile species in the Albertine Rift and their congeners in the Kenyan Highlands (e.g., Tolley et al. 2011, *Kinyongia*; Menegon et al. 2014, *Atheris*).

The major biogeographic feature that seems to separate the geographic distributions of *Adolfus jacksoni* and *A. kibonotensis* is the Kenyan Rift (i.e., Gregory Rift), which divides Kenya in a north–south direction at approximately 36°E longitude, just west of Nairobi and between the Mau Escarpment and the central Kenyan highlands, including the Aberdares and Mt. Kenya (Fig. 1). Several lakes are found along the path of the rift in a north-to-south direction, including Turkana, Logipi, Baringo, Bogoria, Nakuru, Elmenteita, Naivasha, Magadi, and Natron (Chorowicz

2005; Kennedy 2014). Given the stark altitudinal gradients and ecotones represented by the Kenyan Rift, it is not surprising that our study and multiple other ones have demonstrated its importance as a major biogeographic barrier in several plant and animal groups in East Africa. Based on geographic distribution records, the Kenyan Rift has been noted as a barrier to some species of *Lepidochrysoptera* butterflies (de Jong and Congdon 1993), *Rhampholeon* chameleons (Matthee et al. 2004), *Trioceros* chameleons (Spawls et al. 2018), *Thrasops schmidtii* (Spawls et al. 2018), the monotypic viper *Montatheris hindii* (Spawls et al. 2018), *Acomys* mice (Happold 2013), *Arvicanthis* rats (Happold 2013), *Cephalophus* duikers (Kingdon and Hoffmann 2013), and even *Connochaetes* wildebeest (Kingdon and Hoffmann 2013). The rift also seems to be a barrier, at least for some taxa, in DNA-based phylogenies of rodents (Demos et al. 2014a,b, 2015) and *Scotophilus* bats (Demos et al. 2018).

At the microevolutionary scale, several population genetics studies have demonstrated that the Kenyan Rift is a stark barrier to gene flow, including populations of the acacia tree *Senegalia mellifera* (Ruiz Guajardo et al. 2010), *Anopheles gambiae* mosquito (Lehmann et al. 2000), and *Schedorhinotermes lamanius* termite (Wilfert et al. 2006). Moreover, a study of amplified fragment length polymorphisms in the giant lobelia *Lobelia giberroa* (Kebede et al. 2007) recovered distinct groups on each side of the Kenyan Rift (Elgon–Cherangani and Mt. Kenya–Aberdare–Kilimanjaro–Meru). Another study of giant lobelias based on chloroplast DNA restriction analyses (Knox and Palmer 1998) recovered a well-supported clade including populations from Mt. Elgon, Cherangani, and several populations from the Albertine Rift of DRC, Uganda and Rwanda, which is consistent with the phylogeographic pattern we recovered for *Adolfus jacksoni* (Fig. 1) and a similar study of *Dendrosenecio* giant senecios (Knox and Palmer 1995). Bowie et al. (2006) also discovered closely related populations of montane forest robins (*Pogonocichla stellata*) in the Albertine Rift and Kenyan Highlands.

However, some recent studies have shown exceptions to this pattern. For example, Demos et al. (2014b) recovered a clade of *Sylvisorex mundus* forest shrew from both sides of the Kenyan Rift (Mt. Elgon, Cherangani Hills, Mau Escarpment, Mt. Kenya, and the Aberdares), and similar patterns were found in some taxa by Demos et al. (2015). In a multilocus phylogeny of *Scotophilus* bats, Demos et al. (2018) recovered a well-supported lineage (clade 4) from both sides of the rift in southern Kenya. In their study of *Adolfus alleni*, Wagner et al. (2014) recovered a well-supported clade (subsequently named as *A. massavaensis*) with populations from both sides of the Kenyan Rift in Mt. Elgon, Cherangani, and the Aberdares, but some molecular and morphological differences were noted between the populations from the Aberdares and Mt. Elgon (Wagner et al. 2014). Future studies of squamates in East Africa should increase sampling on both sides of the Kenyan Rift to test hypotheses of extinction and dispersal, which might account for these different phylogenetic and distribution patterns.

Compared with other highlands of central Kenya, the biota of the Mathews Range (also erroneously known as the Matthews Range) is poorly known. The site was protected as a forest reserve in 1964, and it is part of the Ewaso ecosystem–landscape of Kenya (Georgiadis 2011). The forested area of the

reserve is approximately 940 km², and because of its remoteness and steep topography, much of the reserve is inaccessible and intact. The reserve is surrounded by the Namunyak Wildlife Conservancy (a member of Northern Rangelands Trust), and people do not live inside the forest. However, the local community (i.e., Samburu pastoralists) enters the reserve with livestock during the dry season, causing overgrazing and damage to branches of evergreen trees where *Adolfus mathewsensis* occurs. Additional environmental damage from honey harvesting (including the use of fire) and firewood collection also occurs in the area (P.K. Malonza, personal observation; Anonymous 2010; de Jong and Butynski 2010). In addition to the new endemic species *A. mathewsensis*, the reserve includes an endemic subspecies of the Kenyan Giant Cycad (*Encephalartos tegulaneus* ssp. *tegulaneus*), some of which may be 600 yr old (Anonymous 2010; Donaldson 2010). The reserve also includes several rare butterflies, five species of primates, one species of montane climbing mouse, one species of *Pipistrellus* bat, and important elephant, lion, and wild dog populations (Anonymous 2010; Georgiadis 2011; Happold 2013; Happold and Happold 2013). Although it is possible that *A. mathewsensis* will be found in proximate montane forest habitats with additional fieldwork efforts (e.g., Ndoto Mountains and Nyiru Range), the species' currently known distribution suggests it is endemic to the Mathews Range. Bowie et al. (2006) noted that the northernmost sites of the Kenyan Highlands, Mt. Kulal and Mt. Marisibit (north and east of the Nyiru Range, respectively) were likely never connected to other mountains, and additional vertebrate endemics should be sought at these sites. Given the relatively small size of the Mathews Range Forest Reserve and the anthropogenic threats to its forests, *A. mathewsensis* will likely be evaluated as threatened with the criteria of the International Union for Conservation of Nature Red List (IUCN 2012).

Acknowledgments.—Fieldwork by the first author in the Democratic Republic of Congo (DRC) was funded by the Percy Sladen Memorial Fund, an International Union for Conservation of Nature/Species Survival Commission Amphibian Specialist Group Seed Grant, K. Reed, research funds from the Department of Biology at Villanova University, a National Geographic Research and Exploration Grant (No. 8556-08), University of Texas at El Paso (UTEP), and a grant from the National Science Foundation (DEB-1145459). EG, CK, MMA, and WMM thank their field companions M. Zigabe, A.M. Marcel, M. Luhumyo, J. and F. Akuku, F.I. Alonda, and the late A. M'Mema. We are grateful to F.B. Murutsi, former Chief Warden of the Itombwe Natural Reserve, for logistical support and permission for fieldwork in 2011; the Centre de Recherche en Sciences Naturelles provided project support and export permits; and we thank the Institut Congolais pour la Conservation de la Nature for permits to work in protected areas in DRC. The Nature Conservancy supported fieldwork by PKM in the Mathews Range in Kenya. PW thanks M. Barej for taking tissues in the Zoologisches Forschungsmuseum Alexander Koenig collection. R. Cody (UTEP) assisted with ARC GIS software to construct the map figure. We acknowledge A. Betancourt of the Border Biomedical Research Center Genomic Analysis Core Facility for services and facilities provided. The Core is supported by Grant G12MD007592 from the National Institutes on Minority Health and Health Disparities, a component of the National Institutes of Health. The findings and conclusions in this article are those of the authors and do not necessarily represent the views of the US Fish and Wildlife Service. All contributors observed appropriate ethical and legal guidelines and regulations, including the American Society of Ichthyologists and Herpetologists—Herpetologists' League—Society for the Study of Amphibians and Reptiles Guidelines for Use of Live Amphibians and Reptiles in Field Research; state, federal, and international laws concerning the collection and transport of preserved specimens; and Institutional Animal Care and Use Committee approval for the care of animals and study procedures used (UTEP IACUC #A-200902-1).

SUPPLEMENTAL MATERIAL

Supplemental material associated with this article can be found online at <https://doi.org/10.1655/HERPMONOGRAPHS-D-18-00005.FS1>; <https://doi.org/10.1655/HERPMONOGRAPHS-D-18-00005.FS2>; <https://doi.org/10.1655/HERPMONOGRAPHS-D-18-00005.TS1>.

LITERATURE CITED

- Anonymous. 2010. Mathews Forest Range Ecological Assessment: Summary Report. Wildlife Conservancy, Samburu, Kenya. Available at <https://www.conservationgateway.org/ConservationByGeography/Africa/Documents/Mathews%20Forest%20Ecological%20Assessment.pdf>. Archived by WebCite at <http://www.webcitation.org/70M2Hdy0b> on 21 June 2018.
- Arnold, E.N. 1973. Relationships of the Palaearctic lizards assigned to the genera *Lacerta*, *Algyroides* and *Psammotromus* (Reptilia: Lacertidae). Bulletin of the British Museum (Natural History), Zoology Series 25:291–366.
- Arnold, E.N. 1989a. Systematics and adaptive radiation of Equatorial African lizards assigned to the genera *Adolfus*, *Bedriagaia*, *Gastropholis*, *Holaspis* and *Lacerta* (Reptilia: Lacertidae). Journal of Natural History 23:525–555.
- Arnold, E.N. 1989b. Towards a phylogeny and biogeography of the Lacertidae: Relationships within an Old-World family of lizards derived from morphology. Bulletin of the British Museum (Natural History), Zoology Series 55:209–257.
- Arnold, E.N., O. Arribas, and S. Carranza. 2007. Systematics of the Palaearctic and Oriental lizard tribe Lacertini (Squamata: Lacertidae: Lacertinae), with descriptions of eight new genera. Zootaxa 1430:1–86. DOI: <https://doi.org/10.11646/zootaxa.1430.1.1>.
- Bandelt, H.-J., P. Forster, and A. Röhl. 1999. Median-joining networks for inferring intraspecific phylogenies. Molecular Biology and Evolution 16:37–48.
- Bauer, A.M., A. de Silva, E. Greenbaum, and T.R. Jackman. 2007. A new species of day gecko from high elevation in Sri Lanka, with a preliminary phylogeny of Sri Lankan *Cnemaspis* (Reptilia: Squamata: Gekkonidae). Mitteilungen aus dem Museum für Naturkunde in Berlin. Zoologische Reihe 83 (Sonderheft):22–32.
- Boulenger, G.A. 1899. Descriptions of two new lizards from the interior of British East Africa. Proceedings of the Zoological Society of London 1899:96–98.
- Boulenger, G.A. 1920. Monograph of the Lacertidae. Volume I. Trustees of the British Museum (Natural History), UK.
- Bowie, R.C.K., J. Fjeldså, S.J. Hackett, J.M. Bates, and T.M. Crowe. 2006. Coalescent models reveal the relative roles of ancestral polymorphism, vicariance, and dispersal in shaping phylogeographic structure of an African montane forest robin. Molecular Phylogenetics and Evolution 38:171–188.
- Bryant, L.J. 1989. Non-dinosaurian lower vertebrates across the Cretaceous–Tertiary boundary in northeastern Montana. University of California Publications in Geological Sciences 134:1–107.
- Cerling, T.E., J.M. Harris, B.J. MacFadden, M.G. Leakey, J. Quade, V. Eisenmann, and J.R. Ehleringer. 1997. Global vegetation change through the Miocene/Pliocene boundary. Nature (London) 389:153–158.
- Chorowicz, J. 2005. The East African rift system. Journal of African Earth Sciences 43:379–410.
- Darriba, D., G.L. Taboada, R. Doallo, and D. Posada. 2012. jModelTest 2: More models, new heuristics and parallel computing. Nature Methods 9:772.
- Davis, J.L., and K.C. Nixon. 1992. Populations, genetic variation, and the delimitation of phylogenetic species. Systematic Biology 41:421–435.
- de Jong, R., and T.C.E. Congdon. 1993. The montane butterflies of the eastern Afrotropics. Pp. 133–172 in Biogeography and Ecology of the Rain Forests of Eastern Africa (J.C. Lovett and S.K. Wasser, eds.). Cambridge University Press, UK.
- de Jong, Y.A., and T. Butynski. 2010. Assessment of the Primates, Large Mammals and Birds of the Mathews Range Forest Reserve, Central Kenya. Eastern Africa Primate Diversity and Conservation Program. The Nature Conservancy, USA. Available at <https://static1.squarespace.com/static/5653e896e4b0a689b3fafd97/t/568f7f92c647adcb23cab25d/1452245154798/De+Jong+%26+Butynski++2010++Mathews+Survey.pdf>. Archived by WebCite at <http://www.webcitation.org/70M2lcN3a> on 21 June 2018.
- de Queiroz, K. 1999. The general lineage concept of species and the defining properties of the species category. Pp. 49–89 in Species: New Interdisciplinary Essays (R.A. Wilson, ed.). Massachusetts Institute of Technology Press, USA.

- de Queiroz, K. 2007. Species concepts and species delimitation. *Systematic Biology* 56:879–886.
- Demos, T.C., B. Agwanda, and M.J. Hickerson. 2014a. Integrative taxonomy within the *Hylomyscus denniae* complex (Rodentia: Muridae) and a new species from Kenya. *Journal of Mammalogy* 95:E1–E15.
- Demos, T.C., J.C. Kerbis Peterhans, B. Agwanda, and M.J. Hickerson. 2014b. Uncovering cryptic diversity and refugial persistence among small mammal lineages across the Eastern Afrotropical biodiversity hotspot. *Molecular Phylogenetics and Evolution* 71:41–54.
- Demos, T.C., J.C. Kerbis Peterhans, T.A. Joseph, J.D. Robinson, B. Agwanda, and M.J. Hickerson. 2015. Comparative population genomics of African montane forest mammals support population persistence across a climatic gradient and Quaternary climatic cycles. *PLoS ONE* 10:e0131800. DOI: <https://doi.org/10.1371/journal.pone.0131800>.
- Demos, T.C., P.W. Webala, M. Bartonjo, and B.C. Patterson. 2018. Hidden diversity of African Yellow House Bats (*Vespertilionidae*, *Scotophilus*): Insights from multilocus phylogenetics and lineage delimitation. *Frontiers in Ecology and Evolution* 6:86.
- Denton, R.K., Jr., and R.C. O'Neill. 1995. *Prototeius stageri*, gen. et sp. nov., a new teiid lizard from the Upper Cretaceous Marshalltown Formation of New Jersey, with a preliminary phylogenetic revision of the Teiidae. *Journal of Vertebrate Paleontology* 15:235–253.
- Donaldson, J.S. 2010. *Encephalartos tegulaneus* subsp. *tegulaneus*. The IUCN Red List of Threatened Species 2010:e.T41913A10592756. Available at <https://doi.org/10.2305/IUCN.UK.2010-3.RLTS.T41913A10592756.en>. Archived by WebCite at <http://www.webcitation.org/70M2xnSpd> on 21 June 2018.
- Drummond, A.J., S.Y.W. Ho, M.J. Phillips, and A. Rambaut. 2006. Relaxed phylogenetics and dating with confidence. *PLoS Biology* 4:e88. DOI: <https://doi.org/10.1371/journal.pbio.0040088>.
- Drummond, A.J., M.A. Suchard, D. Xie, and A. Rambaut. 2012. Bayesian phylogenetics with BEAUti and the BEAST 1.7. *Molecular Biology and Evolution* 29:1969–1973.
- Estes, R. 1964. Fossil vertebrates from the late Cretaceous Lance Formation, eastern Wyoming. University of California Publications in Geological Sciences 49:1–180.
- Evans, S.E. 1998. Crown-group lizards from the Middle Jurassic of Britain. *Palaeontographica A* 250:1–32.
- Evans, S.E. 2003. At the feet of the dinosaurs: The early history and radiation of lizards. *Biological Reviews* 78:513–551.
- Evans, S.E., and Y. Wang. 2005. The Early Cretaceous lizard *Dalinghosaurus* from China. *Acta Palaeontologica Polonica* 50:725–742.
- Excoffier, L., and H.E. Lischer. 2010. Arlequin suite version 3.5: A new series of programs to perform population genetics analyses under Linux and Windows. *Molecular Ecology Resources* 10:564–567.
- Fischer, E., and H. Hinkel. 1992. *Natur Ruandas: Einführung in die Flora und Fauna Ruandas*. Mainz Ministerium des Inneren, Germany.
- Fu, J. 1998. Toward the phylogeny of the Family Lacertidae: Implications from mitochondrial DNA 12S and 16S gene sequences (Reptilia: Squamata). *Molecular Phylogenetics and Evolution* 9:118–130.
- Fu, J. 2000. Toward the phylogeny of the family Lacertidae—Why 4708 base pairs of mtDNA sequences cannot draw the picture. *Biological Journal of the Linnean Society* 71:203–217.
- Georgiadis, N.J. (ed.). 2011. *Conserving Wildlife in African Landscapes: Kenya's Ewaso Ecosystem*. Smithsonian Contributions to Zoology Number 632. Smithsonian Institution Scholarly Press, USA.
- Greenbaum, E., and C. Kusamba. 2012. Conservation implications following the rediscovery of four frog species from the Itombwe Natural Reserve, eastern Democratic Republic of the Congo. *Herpetological Review* 43:253–259.
- Greenbaum, E., C.O. Villanueva, C. Kusamba, M.M. Aristote, and W.R. Branch. 2011. A molecular phylogeny of Equatorial African Lacertidae, with the description of a new genus and species from eastern Democratic Republic of the Congo. *Zoological Journal of the Linnean Society* 163:913–942.
- Greenbaum, E., K.A. Tolley, A. Joma, and C. Kusamba. 2012. A new species of chameleon (Sauria: Chamaeleonidae: *Kinyongia*) from the northern Albertine Rift, Central Africa. *Herpetologica* 68:60–75.
- Greenbaum, E., U. Sinsch, E. Lehr, F. Valdez, and C. Kusamba. 2013. Phylogeography of the reed frog *Hyperolius castaneus* (Anura: Hyperoliidae) from the Albertine Rift of Central Africa: Implications for taxonomy, biogeography and conservation. *Zootaxa* 3731:473–494. DOI: <https://doi.org/10.11646/zootaxa.3731.4.3>.
- Greenbaum, E., F. Portillo, K. Jackson, and C. Kusamba. 2015. A phylogeny of Central African *Boaedon* (Serpentes: Lamprophiidae), with the description of a new species from the Albertine Rift. *African Journal of Herpetology* 64:18–38.
- Groth, J.G., and G.F. Barrowclough. 1999. Basal divergences in birds and the phylogenetic utility of the nuclear RAG-1 gene. *Molecular Phylogenetics and Evolution* 12:115–123.
- Happold, D. (ed.). 2013. *Mammals of Africa, Volume III: Rodents, Hares and Rabbits*. Bloomsbury, UK.
- Happold, M., and D. Happold (eds.). 2013. *Mammals of Africa, Volume IV: Hedgehogs, Shrews and Bats*. Bloomsbury, UK.
- Harris, D.J. 1999. Molecular systematics and evolution of lacertid lizards. *Natura Croatica* 8:161–180.
- Harris, D.J., E.N. Arnold, and R.H. Thomas. 1998. Relationships of lacertid lizards (Reptilia: Lacertidae) estimated from mitochondrial DNA sequences and morphology. *Proceedings of the Royal Society B, Biological Sciences* 265:1939–1948.
- Hipsley, C.A., L. Himmelman, D. Metzler, and J. Müller. 2009. Integration of Bayesian molecular clock methods and fossil-based soft bounds reveals early Cenozoic origin of African lacertid lizards. *BMC Evolutionary Biology* 9:151.
- Huelsenbeck, J.P., and F. Ronquist. 2001. MRBAYES: Bayesian inference of phylogeny. *Bioinformatics* 17:754–755.
- Hughes, D.F., C. Kusamba, M. Behangana, and E. Greenbaum. 2017. Integrative taxonomy of the Central African forest chameleon, *Kinyongia adolfifriederici* (Sauria: Chamaeleonidae), reveals underestimated species diversity in the Albertine Rift. *Zoological Journal of the Linnean Society* 181:400–438.
- Hughes, D.F., K.A. Tolley, M. Behangana, ... E. Greenbaum. 2018. Cryptic diversity in *Rhampholeon boulengeri* (Sauria: Chamaeleonidae), a pygmy chameleon from the Albertine Rift biodiversity hotspot. *Molecular Phylogenetics and Evolution* 122:125–141.
- IUCN [International Union for Conservation of Nature]. 2012. *IUCN Red List Categories and Criteria: Version 3.1., 2nd edition*. IUCN, Switzerland.
- Jones, M.E.H., C.L. Anderson, C.A. Hipsley, J. Müller, S.E. Evans, and R.R. Schoch. 2013. Integration of molecules and new fossils supports a Triassic origin for Lepidosauria (lizards, snakes, and tuatara). *BMC Evolutionary Biology* 13:208.
- Kebede, M., D. Ehrlich, P. Taberlet, S. Nemomissa, and C. Brochmann. 2007. Phylogeography and conservation genetics of a giant lobelia (*Lobelia giberroa*) in Ethiopian and tropical East African mountains. *Molecular Ecology* 16:1233–1243.
- Kennedy, A.S. 2014. *Birds of Kenya's Rift Valley*. Princeton University Press, USA.
- Keqin, G., and M.A. Norell. 2000. Taxonomic composition and systematics of Late Cretaceous lizard assemblages from Ukhaa Tolgod and adjacent localities, Mongolian Gobi Desert. *Bulletin of the American Museum of Natural History* 249:1–118.
- Kingdon, J. 1990. *Island Africa: The Evolution of Africa's Rare Animals and Plants*. Princeton University Press, USA.
- Kingdon, J., and M. Hoffman (Eds.). 2013. *Mammals of Africa, Volume VI: Pigs, Hippopotamuses, Chevrotain, Giraffes, Deer and Bovids*. Bloomsbury, UK.
- Kissling, W.D., W.L. Eiserhardt, W.J. Baker, F. Borchsenius, T.L. Couvreur, H. Balslev, and J.C. Svenning. 2012. Cenozoic imprints on the phylogenetic structure of palm species assemblages worldwide. *Proceedings of the National Academy of Sciences of the United States of America* 109:7379–7384.
- Knox, E.B., and J.D. Palmer. 1995. Chloroplast DNA variation and the recent radiation of the giant senecios (Asteraceae) on the tall mountains of eastern Africa. *Proceedings of the National Academy of Sciences of the United States of America* 92:10349–10353.
- Knox, E.B., and J.D. Palmer. 1998. Chloroplast DNA evidence on the origin and radiation of the giant lobelias in Eastern Africa. *Systematic Botany* 23:109–149.
- Köhler, J., P. Wagner, S. Visser, and W. Böhme. 2003. New country records of *Adolfus africanus* (Sauria: Lacertidae)—A rain forest lizard with disjunct distribution? *Salamandra* 39:241–248.
- Larson, T., D. Castro, M. Behangana, and E. Greenbaum. 2016. Evolutionary history of the river frog genus *Amietia* (Anura: Pyxicephalidae) reveals extensive diversification in Central African highlands. *Molecular Phylogenetics and Evolution* 99:168–181.
- Leaché, A.D., and T.W. Reeder. 2002. Molecular systematics of the eastern fence lizard (*Sceloporus undulatus*): A comparison of parsimony, likelihood, and Bayesian approaches. *Systematic Biology* 51:44–68.
- Lehmann, T., C.R. Blackston, N.J. Besansky, A.A. Escalante, F.H. Collins, and W.A. Hawley. 2000. The Rift Valley Complex as a barrier to gene flow

- for *Anopheles gambiae* in Kenya: The mtDNA perspective. *Journal of Heredity* 91:165–168.
- Leigh, J.W., and D. Bryant. 2015. POPART: Full-feature software for haplotype network construction. *Methods in Ecology and Evolution* 6:1110–1116.
- Librado, P., and J. Rozas. 2009. DnaSP v5: A software for comprehensive analysis of DNA polymorphism data. *Bioinformatics* 25:1451–1452.
- Lönnberg, E. 1907 [1910]. Reptilia and Batrachia. Pp. 1–28 in *Wissenschaftliche Ergebnisse der Schwedischen Zoologischen Expedition nach dem Kilimandjaro, dem Meru und dem umgebenen Massaiesteppen 1905–1906* (Y. Sjostedt, ed.). P. Palmquist, Sweden.
- Loveridge, A. 1957. Check list of the reptiles and amphibians of East Africa (Uganda; Kenya; Tanganyika; Zanzibar). *Bulletin of the Museum of Comparative Zoology, Harvard* 117:153–362, xxxvi.
- Lue, K.-Y., and S.-M. Lin. 2008. Two new cryptic species of *Takydromus* (Squamata: Lacertidae) from Taiwan. *Herpetologica* 64:379–395.
- Maddison, D.R., and W.P. Maddison. 2005. *MacClade: Analysis of Phylogeny and Character Evolution*. Sinauer Associates, Inc., USA.
- Matthee, C.A., C.R. Tilbury, and T. Townsend. 2004. A phylogenetic review of the African leaf chameleons: Genus *Rhampholeon* (Chamaeleonidae): The role of vicariance and climate change in speciation. *Proceedings of the Royal Society B: Biological Sciences* 271:1967–1975.
- Mayer, W., and M. Pavlicev. 2007. The phylogeny of the family Lacertidae (Reptilia) based on nuclear DNA sequences: Convergent adaptations to arid habitats within the subfamily Eremiinae. *Molecular Phylogenetics and Evolution* 44:1155–1163.
- Mendes, J., D.J. Harris, S. Carranza, and D. Salvi. 2016. Evaluating the phylogenetic signal limit from mitogenomes, slow evolving nuclear genes, and the concatenation approach: New insights into the Lacertini radiation using fast evolving nuclear genes and species trees. *Molecular Phylogenetics and Evolution* 100:254–267.
- Mendes, J., D. Salvi, D.J. Harris, J. Els, and S. Carranza. 2018. Hidden in the Arabian Mountains: Multilocus phylogeny reveals cryptic diversity in the endemic *Omanosaura* lizards. *Journal of Zoological Systematics and Evolutionary Research* 56:395–407.
- Menegon, M., S.P. Loader, S.J. Marsden, W.R. Branch, T.R.B. Davenport, and S. Ursenbacher. 2014. The genus *Atheris* (Serpentes: Viperidae) in East Africa: Phylogeny and the role of rifting and climate in shaping the current pattern of species diversity. *Molecular Phylogenetics and Evolution* 79:12–22.
- Packard, G.C., and T.J. Boardman. 1999. The use of percentages and size-specific indices to normalize physiological data for variation in body size: Wasted time, wasted effort? *Comparative Biochemistry and Physiology Part A* 122:37–44.
- Palumbi, S., A. Martin, S. Romano, W.O. McMillan, L. Stice, and G. Grabowski. 1991. *The Simple Fool's Guide to PCR, Version 2*. The University of Hawaii, USA.
- Pavlicev, M., and W. Mayer. 2006. Multiple copies of coding as well as pseudogene c-mos sequence exist in three lacertid species. *Journal of Experimental Zoology Part B Molecular and Developmental Evolution* 306B:539–550.
- Pavlicev, M., and W. Mayer. 2009. Fast radiation of the subfamily Lacertinae (Reptilia: Lacertidae): History or methodical artefact? *Molecular Phylogenetics and Evolution* 52:727–734.
- Peters, J.A. 1964. *Dictionary of Herpetology*. Hafner Publishing Company, USA and UK.
- Poblete, G.H. 2002. *Adolfus jacksoni* Boulenger 1899. Jackson's lizard. *Morphology. African Herp News* 34:23–24.
- Portillo, F., E. Greenbaum, M. Menegon, C. Kusamba, and J.M. Dehling. 2015. Phylogeography and species boundaries of *Leptopelis* (Anura: Arthroleptidae) from the Albertine Rift. *Molecular Phylogenetics and Evolution* 82:75–86.
- Portillo, F., W.R. Branch, W. Conradie, ... E. Greenbaum. 2018. Phylogeny and biogeography of the African burrowing snake subfamily Aparallactinae (Squamata: Lamprophiidae). *Molecular Phylogenetics and Evolution* 127:288–303.
- Posada, D., and T.R. Buckley. 2004. Model selection and model averaging in phylogenetics: Advantages of Akaike information criterion and Bayesian approaches over likelihood ratio tests. *Systematic Biology* 53:793–808.
- Rambaut, A., and A. Drummond. 2010. *FigTree, Version 1.3.1*. Institute of Evolutionary Biology, University of Edinburgh, UK. Available at <http://tree.bio.ed.ac.uk/software/figtree/>. Archived by WebCite at <http://www.webcitation.org/70M3Y2HLb> on 21 June 2018.
- Ronquist, F., and J.P. Huelsenbeck. 2003. MRBAYES 3: Bayesian phylogenetic inference under mixed models. *Bioinformatics* 19:1572–1574.
- Ruiz Guajardo, J.C., A. Schnabel, R. Ennos, S. Preuss, A. Otero-Araiz, and G. Stone. 2010. Landscape genetics of the key African acacia species *Senegalia mellifera* (Vahl): The importance of the Kenyan Rift Valley. *Molecular Ecology* 19:5126–5139.
- Sabaj, M.H. 2016. *Standard Symbolic Codes for Institutional Resource Collections in Herpetology and Ichthyology: An Online Reference, Version 6.5*. American Society of Ichthyologists and Herpetologists, USA. Available at <http://www.asih.org/>. Archived by WebCite at <http://www.webcitation.org/70M20xvyS> on 21 June 2018.
- Salvi, D., P. Bombi, and L. Vignoli. 2011. Phylogenetic position of the southern rock lizard *Australolacerta australis* within the Lacertidae radiation. *African Journal of Herpetology* 60:60–69.
- Sepulchre, P., G. Ramstein, F. Fluteau, M. Schuster, J.J. Tiercelin, and M. Brunet. 2006. Tectonic uplift and Eastern Africa aridification. *Science (Washington)* 313:1419–1423.
- Spawls, S., K. Howell, H. Hinkel, and M. Menegon. 2018. *Field Guide to East African Reptiles*, 2nd edition. Bloomsbury, UK.
- Stamatakis, A. 2006. RAXML-VI-HPC: Maximum likelihood-based phylogenetic analyses with thousands of taxa and mixed models. *Bioinformatics* 22:2688–2690.
- Stamatakis, A., F. Blagojevic, D. Nikolopoulos, and C. Antonopoulos. 2007. Exploring new search algorithms and hardware for phylogenetics: RAXML meets the IBM cell. *Journal of VLSI Signal Processing* 48:271–286.
- Stamatakis, A., P. Hoover, and J. Rougemont. 2008. A rapid bootstrap algorithm for the RAXML web servers. *Systematic Biology* 57:758–771.
- Stephens, M., and P. Donnelly. 2003. A comparison of Bayesian methods for haplotype reconstruction from population genotype data. *The American Journal of Human Genetics* 73:1162–1169.
- Sternfeld, R. 1912 [1913]. Reptilia. Pp. 197–279 + Figs. 1–4 + Pl. VI–IX in *Wissenschaftliche Ergebnisse der Deutschen Zentral-Afrika-Expedition 1907–1908 unter Führung Adolf Friedrichs, Herzogs zu Mecklenburg. Band IV, Zoologie II*. Klinkhardt and Biermann, Germany.
- Sullivan, R.M., and S. G. Lucas. 1996. *Palaeoscincosaurus middletoni*, new genus and species (Squamata: Scincidae) from the Early Paleocene (Pueran) Denver Formation, Colorado. *Journal of Vertebrate Paleontology* 16:666–672.
- Swindell, S.R., and T.N. Plasterer. 1997. SEQMAN: Contig assembly. *Methods in Molecular Biology* 70:75–89.
- Tamura, K., G. Stecher, D. Peterson, A. Filipski, and S. Kumar. 2013. MEGA6: Molecular evolutionary genetics analysis version 6.0. *Molecular Biology and Evolution* 30:2725–2729.
- Thompson, J.D., D.G. Higgins, and T.J. Gibson. 1994. CLUSTAL W: Improving the sensitivity of progressive multiple sequence alignment through sequence weighting, position-specific gap penalties and weight matrix choice. *Nucleic Acids Research* 22:4673–4680.
- Tolley, K.A., C.R. Tilbury, G.J. Measey, M. Menegon, W.R. Branch, and C.A. Matthee. 2011. Ancient forest fragmentation or recent radiation? Testing refugial speciation models in chameleons within an African biodiversity hotspot. *Journal of Biogeography* 38:1748–1760.
- Wagner, P., E. Greenbaum, P. Malonza, and W.R. Branch. 2014. Resolving sky island speciation in populations of East African *Adolfus alleni* (Sauria, Lacertidae). *Salamandra* 50:1–17.
- Wiens, J.J., and T.A. Penkrot. 2002. Delimiting species using DNA and morphological variation and discordant species limits in spiny lizards (*Sceloporus*). *Systematic Biology* 51:69–91.
- Wilcox, T.P., D.J. Zwickl, T.A. Heath, and D.M. Hillis. 2002. Phylogenetic relationships of the dwarf boas and a comparison of Bayesian and bootstrap measures of phylogenetic support. *Molecular Phylogenetics and Evolution* 25:361–371.
- Wilfert, L., M. Kaib, W. Durka, and R. Brandl. 2006. Differentiation between populations of a termite in eastern Africa: Implications for biogeography. *Journal of Biogeography* 33:1993–2000.
- Zheng, Y., and J.J. Wiens. 2016. Combining phylogenomic and supermatrix approaches, and a time-calibrated phylogeny for squamate reptiles (lizards and snakes) based on 52 genes and 4162 species. *Molecular Phylogenetics and Evolution* 94:537–547.

APPENDIX I Voucher numbers, localities, and GenBank accession numbers for new genetic samples sequenced for this study. DRC = Democratic Republic of the Congo, NP = national park. See Materials and Methods for collection abbreviations.

Species	Collection No.	Field No.	Locality	16S	cyt b	c-mos	RAG1
<i>Adolfus jacksoni</i>	ZFMK 81966	MB 328	KENYA: Kakamega: Kakamega Forest	MH891083	MH891093	MH891104	MH891115
<i>Adolfus jacksoni</i>	ZFMK 81971	MB 331	KENYA: Kakamega: Kakamega Forest	MH891082	MH891092	MH891103	MH891114
<i>Adolfus jacksoni</i>	ZFMK 88169	MB 335	RWANDA: Northern: Ruhengeri	MH891085	MH891095	MH891106	MH891116
<i>Adolfus jacksoni</i>	ZFMK 63360	MB 338	UGANDA: Western: Fort Portal	MH891086	MH891096	MH891107	MH891117
<i>Adolfus jacksoni</i>	ZFMK 63264	MB 341	UGANDA: Western: Rwenzori Mountains NP, Kilembe	MH891081	MH891091	MH891102	MH891113
<i>Adolfus jacksoni</i>	ZFMK 63267	MB 342	UGANDA: Western: Rwenzori Mountains NP, Kilembe	MH891087	MH891097	MH891108	—
<i>Adolfus jacksoni</i>	ZFMK 74512	MB 346	UGANDA: Eastern: Mt. Elgon: Bujitimwa	MH891084	MH891094	MH891105	—
<i>Adolfus kibonotensis</i>	—	NMK H-172	KENYA: Taita: Taita-Taveta: Ngulia Hills, Tsavo West NP	MH891079	MH891090	MH891100	MH891111
<i>Adolfus kibonotensis</i>	NMK L3203	PKM 287	KENYA: Nairobi: Nairobi, City Park Forest	MH891078	MH891089	MH891099	MH891110
<i>Adolfus kibonotensis</i>	NMK L/3190	NMK H-50	KENYA: Meru South: Mt. Kenya: Chogoria forest block	MH891077	MH891088	MH891098	MH891109
<i>Adolfus matheusensis</i>	NMK L/3376/2	PKM 239	KENYA: Samburu: Mathews Range North: Mugur Base Camp area, Ng'eny Riverine forest, near Kitich Camp	MH891080	—	MH891101	MH891112

APPENDIX II

Additional Specimens Examined

Adolfus jacksoni (30).—DEMOCRATIC REPUBLIC OF THE CONGO: ITURI: Lendu Plateau, Mt. Aboro, 02.0094°N, 30.8651°E, 2445 m (UTEF 20285–86), Aboro, 02.00587°N, 30.8352°E, 2065 m (UTEF 20282–84). SOUTH KIVU: Kahuzi-Biega National Park, Tshivanga, 02.3128°S, 28.7552°E, 2200 m (UTEF 20272–73), Kahuzi-Biega National Park, Mugaba, 02.27301°S, 28.65862°E, 2290 m (UTEF 20278), Lwiro, 02.2384°S, 28.8052°E, 1750 m (UTEF 20275), east of Lwiro, 02.24099°S, 28.84962°E, (UTEF 20277), Itombwe Plateau, Kizuka, 03.00658°S, 28.75005°E, 2450 m (UTEF 20280). KENYA: RIFT VALLEY: Bomet County: South-Western Mau National Reserve, Kipteket River, 00°30'S, 35°20'E (NMK L/1919). Nakuru County: Subukia, 7000 ft (2134 m; FMNH 78666), East Mau Forest, Kipsaungon (NMK L/1992/2,5,6), Njoro (FMNH 58289–90), Njoro, 7500 ft (2286 m; FMNH 78667). West Pokot County: Lotongot, 01.733333°N, 35.633333°E (LACM 60798). Trans Nzoia County: Cherangani Mountains, Kapchorop, 01.033333°N, 35.316667°E, 2134 m (LACM 60858–59). Narok County: “Loita Plains, Mau Esc.[arpmnt] KC” 01.25°S, 35.58333333°E (MCZ R-17990). NYANZA: Kisumu County: Chemelil,

00°6'0"S, 35°7'0"E (CAS 152783). WESTERN: Bungoma County: South Mt. Elgon, Elgoni (MCZ R-41152–53). Kakamega County: Kakamega Forest, near Kaimosi, 00°12'20"N, 34°29'30"E (CAS 122729). UGANDA: CENTRAL: Masaka District: Lake Nabagabo, 00°22'0"S, 31°52'0"E (CAS 204386). WESTERN: Kabale District: Bwindi Impenetrable National Park, Kabale-Kayonza road, 01°2'36.8"S, 29°46'5.4"E, 7700 ft (2347 m; CAS 201610), Bwindi Impenetrable National Park, Institute for Tropical Forest Conservation, Ruhizha, 01°2'47.8"S, 29°46'28.5"E, 7750 ft (2362 m; CAS 201598).

Adolfus kibonotensis (10).—KENYA: COAST: Taita-Taveta County, Taita Hills, Mt. Mbololo, 03.28333333°S, 38.46666667°E (MCZ R-41169), Taita Hills, Chawia Forest, 03°28'26.28"S, 38°29'57.7"E, 1610 m (NMK L/2350), Taita Hills, Mwachora Forest, 03°24'57.99"S, 38°22'6.16"E, 1644 m (NMK L/2224/1–2), Taita Hills, Macha Forest, 03°25'3.69"S, 38°21'31.35"E, 1650 m (NMK L/2223/2), Taita Hills, Mwambirwa forest plantation, 03°20'45.59"S, 38°25'39.42"E, 1300 m (NMK L/2879). EASTERN: Meru District: Kairuni, 00.183333°N, 37.866667°E (LACM 93307–08), Mt. Kenya Forest, Chogoria forest route, 00°12'27.4"S, 37°29'57.7"E, 2402 m (NMK L/3190). NAIROBI: Nairobi County: Nairobi City Park forest, 01°15.998'S, 36°49.586'E, 1661 m (NMK L/3203).